Faculdade de Engenharia da Universidade do Porto

Intelligent Skin for Self-Powered Hand Motion Sensing Based on Triboelectric Nanomaterials

Rogério Fernando Cruz Ribeiro

September, 2020

Faculdade de Engenharia da Universidade do Porto

Intelligent Skin for Self-Powered Hand Motion Sensing Based on Triboelectric Nanomaterials

Rogério Fernando Cruz Ribeiro

Dissertação realizada no âmbito do

Mestrado em Engenharia Biomédica

Orientador: Prof. João Ventura

September, 2020

Resumo

Esta dissertação apresenta um protótipo que visa o reconhecimento de padrões na superfície de materiais com recurso ao efeito triboelétrico. Desta forma foram amadurecidos os conhecimentos nas diferentes estratégias de produção autónoma de energia, equipamentos que são utilizados no dia -a-adia que recorrem a estas estratégia, tanto no que se refere a conhecimento de formas de conversão, como à adaptação destas estratégias ao desempenho de funções de sensores atualmente existentes no mercado.

Assim, com recurso a tecnologias quotidianas, esta dissertação retrata o desenvolvimento de um sensor autossuficiente, com recurso ao efeito triboelétrico para obtenção da posição relativa entre dois segmentos contíguos dos dedos da mão. Tendo por base o funcionamento de um encoder absoluto, foi desenvolvido um sensor com 7 bits e 2,81º de resolução em código Gray. Para isso e como forma de auxiliar e validar os dados obtidos, foram modelados e desenvolvidos os dispositivos para esse efeito.

Atendendo ao que foi desenvolvido e estudado durante esta dissertação, o efeito triboelétrico pode ser utilizado para o reconhecimento de padrões na superfície de materiais e posteriormente indicador da posição exata de uma estrutura em relação a outra.

Esta dissertação pode ser consultada online no website [1], ou mesmo no artigo resumo que foi submetido com a mesma.

Palavras-chave: Encoder, pele-eletrónica, sensor, triboelétrico

Abstract

This dissertation presents a prototype that aims to monitor patterns on surfaces using the triboelectric effect. Thus, knowledge was solidified regarding self-powered energy production strategies such as devices that use this technology and are used in everyday life. Forms of conversion and adaptation of these same strategies were also known so that they could perform the functions of sensors currently on the market without recourse to external energy sources.

Thus, through everyday technologies this dissertation focuses on the development of a self-powered sensor using the triboelectric effect to obtain the relative position between two contiguous segments of the hand. Based on the principle of operation of an absolute encoder, a sensor with 7 bits and 2.81º resolution in Gray code was developed. For this and as a way of aiding and validating the data that were obtained, devices were developed capable of assisting in the validation and achievement of the desired results using 3D printing, software development as well as the programming of microcontrollers.

So, using the devices developed, through the fundamentals that have been studied and by the data obtained the triboelectric nanogenerators can be used for recognition of surface patterns and subsequently indicators of the exact position of a structure in relation to the other common post processing that can be considered real time, as indicated in the objective of this dissertation.

This dissertation could be followed at the website presented at the link at the references [1].

Keywords: Electronic skin, encoder, sensor, triboelectric

Acknowledgement

First of all, I would like to thank you for the effort made for the development of this dissertation to Cátia Rodrigues with whom I learned a lot. Many thanks also to Professor Dr. João Ventura for helping me organize the ideas and for the patience in trying to understand my lines of thought. To the entire team of inanoEnergy, Diego, Ricardo and the tireless José, thank you very much.

To the members of IFIMUP who throughout this year and a half followed my work and that I could see the work that is developed by them especially to Ana Pires, Catarina Dias, Rita Veloso and Sofia Caspani, Tiago Leal and Joao Fredet.

To Pedro for the indeterminable doubts about the brave world of electronics and Laura Apolinário by the company and help during the development of the whole dissertation.

Lastly and with great affection, a sincere thanks to my favorite psychologist, friends and family.

Contents

Figure Index

Table index

Abreviations, acrinyms and symbols

E-skin	Electronic Skin
TENG	Triboelectric Nanogenerators
PTFE	Polytetrafluoroethylene (Teflon)
PE	Polyethylene
PDMS	Demitilpolissiloxane
.stl	stereolithography
.txt	Text file

m	meter
mm	milimiters
mms^{-1}	milimiters for second

Chapter 1 - Introduction

In this chapter will be made a short introduction related to electronic skins, the motivation for the development of this dissertation as well as the objectives that are intended to achieve.

1. Context

Over time humans has been developing different energy production strategies. This energy production can be carried out sustainably in wind power plants, dams or using classic methods such as nuclear power plants, power plants through coal, etc. However, autonomous energy production methods have been the subject of special interest by researchers, being considered low cost and easy to implement serving different purposes. These methods are used to power sensors that use low currents or even being used as sensors in various applications.

Autonomous methods of energy production use physical principles such as thermoelectric, piezoelectric, triboelectric and others. The orientation of electrical charges in each direction allows the obtaining of currents and potential differences that can be used as a power supply of sensors or used as sensors depending on the medium in which they are inserted.

In biomedical instrumentation the implementation of sensors that allow the analysis of the most diverse human patterns in a noninvasive way has been the focus of technological development in this area. Thus, the development of increasingly small sensors or even the implementation of strategies that do not require the constant monitoring of these devices allow the attribution of a better quality of life to those who use them.

1.1. Motivation

The development of tools capable of monitoring different variables, such as speed, acceleration, distance, pressure, deformation, among others, has been the focus of researchers, keeping the performance of their devices, lowering energy consumption by these sensors. To reduce energy consumption several strategies were studied. Those use a known self-powered strategy principle such as thermoelectric, piezoelectric and triboelectric effect to fabricate sensors capable to be implemented at some environment and output data or even source other sensor by electrical current.

In medical instrumentation, the existence of sensors that allow monitoring the different human anatomical regions are responsible for better knowledge of the patterns inherent to the human being, as well as the development of strategies capable of providing a better life quality after an intervention or even the improvement of some physical aspect. Integrating a self-power sensor into an electronic skin will provide a low consumption by that gadget and the exam could last longer.

2. Objective

Health care monitoring has receive such special attention from the human being that every device such as smartwatches, smartphones and others as the skill to analyze physiological parameters like hearth beats, based on a light sensor that counts the pulses at a located vessel , travelled distance, using a GPS locator, calculating the steps that were taken based on the inertia sensor. Companies have been developing wearables with different sensors to monitor human patterns. Implementing several sensors at a known region capable to analyze some variables is known as electronic skin. So, using this kind of sensors let some space to monitoring hand motion.

The objective of this dissertation is to develop a sensor capable of monitoring the absolute position of two contiguous segments of the fingers of the hand. To achieve this objective, knowledge of the principles of use and implementation of TENG is first necessary. The development of material equipment that allow the progression of the project.

Chapter 2 – Self powered sensors and monitoring strategies

In this chapter will be made a brief introduction on the fundamental concepts related to electronic-skins (e-skins), principles of operation, implementation strategies, self-power sensors based on triboelectric nanogenerators (TENGs) and action focusing on what will be developed in this dissertation.

1. Electronic skins

Over time the quantification of a given parameter in each function has gained increasing interest on the part of researchers. Quantification and monitoring of structures have evolved the classical electronics creating increasingly small sensors and with multimodal capacity, quantification of different variables. In the field of medical instrumentation, the development of devices that allow analysis and knowledge of human patterns are very ambitious. E-skins are devices built with sensors that allow the analysis of different variables such as sweat pH, blood oxygen rate, respiratory cycles, heart rate, among other variables, depending on the region where they are located (Figure 1).

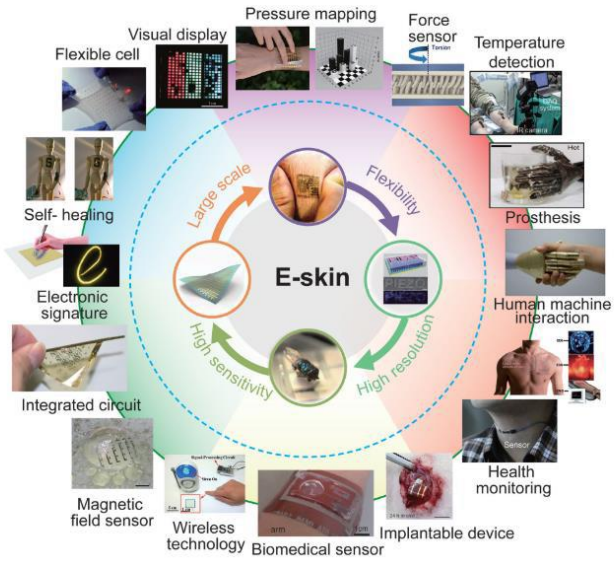

Figure 1. Diverse function and application of sensor devices integrating a multimodal e-skin [2]

1.1. Implementation and data collection

To analyse different human patterns requires the use of several sensors, that use different physical principles to convert the variable that we are studying to an electrical signal to be interpreted by an acquisition device. As examples, an extensometer, as shown in the Figure 2, use a variable resistance principal, which is proportional to the displacement, a thermocouples, uses two different materials and a reference probe in order to measure a temperature, based on the difference of potential from the other probe. These kinds of principles are used to obtain electrophysiological signals, respiratory, cycle, movement of body structures, temperature and deformation among others as reported by Kaichen Xu et al[3]. To keep the reproducibility of several test, it is important that the followed pattern is commonly used by several research groups, as an example is the 10-20 pattern in electroencephalography or the electrode position to electrocardiography and electromyography.

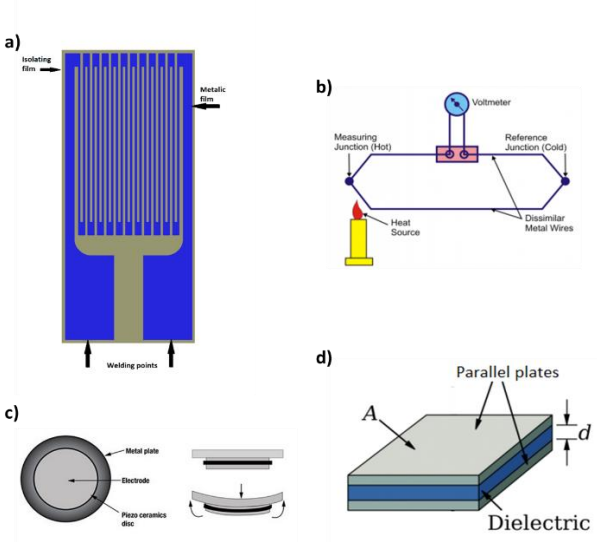

Figure 2. Types of sensors: a) Resistive sensor, extensometer; b) Thermocouple schematics; c) Piezoelectric sensor; d) Parallel plate capacity, A- area, d- distance between parallel plates

1.1.1. Resistive sensor

Resistive sensor like the ones who output voltage depending on the displacement of the material caused by external forces show the flowing relation:

$$\varepsilon = \frac{\Delta L}{L}$$

where ΔL represents the displacement depending on the length of rest L so that deformation ε is obtained. In the manufacture of these sensors is used a thin insulating coating that supports the metallic film that incorporates a pattern. On the side of the metal surface this includes an adhesive to adhere to the area where the displacement measurement is intended [4]

Strength variation of a material depends not only on its length but on the cross section and resistivity itself, those are parameters that will influence the final value of the resistance of the material.

$$R = \rho \cdot \frac{L}{S}$$

representing ρ the resistivity of the material, L the length and S the cross-section of the material [4].

1.1.2. Capacitive sensors

This kind of sensor are built by two electrical conductors separated by a dielectric material. The number of loads is given by:

$$Q = C \cdot V$$

where V represents the voltage to the terminals of the C capacity of the capacitor. Its capacity is calculated using:

$$C = \varepsilon_0 \cdot \varepsilon_r \cdot \frac{A}{d}$$

Where A represents the useful area formed by the metal plates at distance d, ε_0 is the electrical primitiveness in the void, being followed by thee dielectric constant ε_r of the medium separating the two plates [4].

1.1.3. Inductive sensors

Inductive sensors are used for displacement measurements, counting rates, or even tracking an object. In medical context are used for heart volume measurement, breath monitoring and checking the diameter of blood vessels. Its inductance is related to the number of coil sneezing. Generically the inductance is expressed by:

$$L = K_f \cdot N \cdot \mu$$

where K_f is the parameter associated with the geometric shape of the coil, N the number of spirals and μ is the magnetic permeability of the core [4].

1.1.4. Piezoelectric sensors

Piezoelectricity defines the ability of a crystalline material to generate electrical current in reaction to mechanical deformation. It is possible to establish a relationship between the deformation of the material and the intensity of the electric field generated. By ceasing the force molecular loads return to the initial positions. During the time of return to the initial positions,

there is a current in reverse and of equal value to the flow. The piezoelectric effect predominates in crystalline materials, namely quartz, Rochelle salt, some types of ceramics and polymers (such as vinylide polyfluoride, PVDF) [4].

Piezoelectric sensors use the same principles as capacitive sensors. The Q load that is accumulated on the surface depends on the applied force F and the piezoelectric constant K_p of the material [4]:

$$Q = F \cdot K_p$$

The capacity of parallel plates is given by:

$$C_p = \varepsilon \cdot \frac{A}{d}$$

where ε represents the dielectric constant of the material, A the area of the electrodes and d the distance between the electrodes [4].

1.1.5. Thermoelectric sensors

There are several devices and phenomena to measure temperature. Thermocouples, temperature-dependent resistances, thermistors and thermometry are examples of temperature-related sensors.

The thermocouple generates a potential difference that will depend on the temperature difference between the ends of the materials pair used. This strategy will depend on the Seebeck coefficient of each of the materials used. The output voltage by the thermocouple is given by the following equation:

$$V_{out} = (\alpha_A - \alpha_B) \cdot (T_1 - T_2)$$

where V_{out} represents the output voltage between the different materials, $(\alpha_A - \alpha_B)$ indicates the difference between the Seebeck coefficients of the two materials used and the temperature difference between the ends of the materials $(T_1 - T_2)$ [4].

Thermistors are used in combination with resistance to measure temperature values. Thermistors are semiconductor materials consisting of crystalline metal oxides. These materials can be distinguished into two types, PTC (Positive Temperature Coefficient) or NTC (Negative Temperature Coefficient). NTC-type thermistors are the most used because they present resistance variations from a given threshold temperature, implying that they are easier to handle [4].

Temperature-dependent resistances are commonly known as RTD. These are like thermal stores, have variation in resistance with temperature, with the difference being relative to

manufacturing. The thermistors use metal elements, and the most used materials for the construction of RTDs are copper, nickel and platinum. RTD should be an integral part of a Wheatstone bridge in order to increase their sensitivity by the changing of resistance [4].

Radiation thermometry allows you to measure the temperature of a body without having to be in contact with it. This method takes advantage of the relationship between radiation emitted by the body and the surface temperature of the body. This technique allows obtaining temperature maps along the body surface, being possible to diagnose different pathologies such as breast cancer. As a fundamental principle, this technique uses Stefan-Boltzman's law following Wien's law to present the maximum wavelength to a given temperature θ. This kind of principle is used by biomedical systems in auricular thermometer [4].

1.1.6. Magnetic sensors for Hall effect

The Hall effect arises when an electrical current propagates in a conductor in the presence of an external magnetic field. The electric current being the orderly and oriented propagation of electrical charges when subjected to a magnetic field perpendicular to its direction of motion generate the Lorentz's force that will follow the right-hand rule. This force will increase the number of charges perpendicular to the electrical and magnetic field [4] [5].

The Hall effect is the most common method for measuring magnetic fields being typically used in inductive sensors. These devices incorporate high-gain sensors due to the low potential differences that are generated through Lorentz's strength. Sensors that use this strategy can be classified into two types. Analogy, being used to measure distances, due to the constant relationship of the output as a function of the magnetic field. Digital, requiring the use of a Schmitt trigger, with the aim of being regulated the threshold to obtain the output ON. This type of sensors is used in 3D printers, CNC's, detection and positioning and in the automation industry [5], [6].

1.1.7. Optic fiber sensors

Optical fiber sensors, unlike the sensors mentioned above, have the particularity of not suffering interference from parasite electromagnetic noise. These are based on the injection of an infrared beam of light that will propagate along the length of the fiber optic cable being reflected to the end of the conductor. The beam of light changes in its amplitude and frequency according to the information that is required to be transported. Optical fiber can incorporate two distinctions, being conventional, integrating devices that will be based on the evaluation of infrared light beam attenuation as is the case of the straps used for monitoring the respiratory cycle. Optical fibers with Bragg networks compared to conventional optical fibers are a better option for incorporation into sensors due to their higher sensitivity. According to the bibliography these can be used to

measure various quantities, namely deformation, pressure, acceleration, temperature, tilt angles, humidity and intensity of magnetic fields [4].

1.1.8. Optical sensors

The most used optical method for measuring chemical components is absorption spectrometry. Spectrometry allows monitoring the concentration of compounds in the blood, such as glucose, uric acid, lipoproteins, among others.

A spectrometer measures amplitude intensity in their wavelengths. The spectrometer is based on the Beer-Lambert law that allows, by the incision of a light beam, obtaining the concentration of a chemical component as well as the path travelled by this luminous beam [4]

$$A = A_0 \cdot e^{-K_c \cdot C \cdot d}$$

where A_0 is the intensity of the incident light in the cuvet, A is the intensity of light after transmission through cuvet and C is the concentration of the absorbent substance, K_c the proportionality constant and d the length of the optical path [4].

1.2. Data processing and intrepretation

As already mentioned, data collection must comply with several parameters to make it possible to compare them and test their veracity. The sensors present in the e-skins can be passive or active, being possible or not to obtain results directly without the need for processing. However, with technological evolution, data obtained through the most different means such as surveys, electrical signals, among others, are processed through statistical methods that are increasingly common when it comes to data processing. Currently, the large databases of signals, images and others have provided the analysis of common patterns and it is possible to train a neuronal network capable of interpreting situations related to these same data, managing to assign a diagnosis. The trouble with this machine learning processes are located at the amount of data that is needed to train its accuracy.

With a short dataset it is possible to obtain some information too, applying several processes such as normalization, standardization or using a crossing-zero functions this are statistical processes to interpret data. Filters could be used directly on the electrical circuit or even at the post-processing using some software.

2. Triboelectrification

The sharing of electrical charges across the surface of two materials is at the base of the triboelectric effect. These materials are classified through their relative polarity being integral members in a series (Figure 3) ordered by that same property. At the top of this are the materials loaded more positively and, in the end, that are more negative. The selection of the pair of

triboelectric materials is carried out according to the distance that exists between them in this classification. This distance is directly related to the sharing of charges between these two materials, the greater the distance the greater the difference of potentials, and amount of charges that will be shared between them in order to maintain the electrostatic balance in their contact.

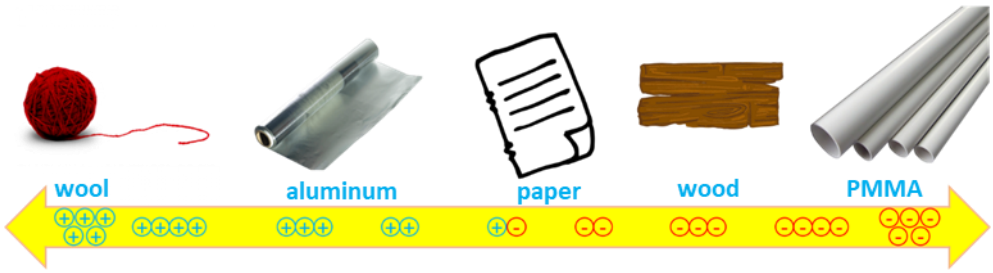

Figure 3. Triboelectric series

2.1.Implementation methods

The sharing of electrical charges in triboelectric materials occurs when a pair of materials establishes physical contact or is very close to each other. In view of this, different principles of operation were studied (Figure 4).

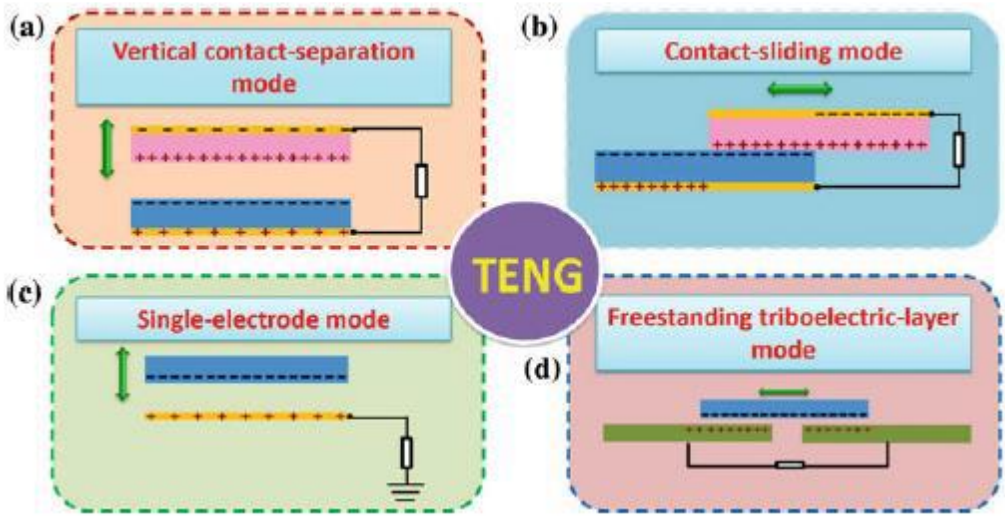

Figure 4. TENG operation principles. a) contact separation mode; b) sliding mode; c) single electrode mode; d) freestanding mode.

The main modes of operation are the vertical contact and contact-sliding one, their operating principle has been adapted to situations in which it is not possible to implement them originating the single electrode and freestanding layer methods. When the materials are away the potential difference corresponds to the difference of charges existing on the surface of the two electrodes. At the time the electrodes establish contact, charges are shared maintaining electrostatic balance, consequently the potential difference is zero.

The principles that were previously analyzed can be used for positioning monitoring on an incremental method, reported by Ya Yang et al. [7]. This method allows you to graphically obtain the position through a reference and with a view of a maximum in an oscillation on the graph (Figure 5). It is also noticeable the orientation of the progression that we are analyzing using graphic analysis through the concavity of the pike that is sampled graphically.

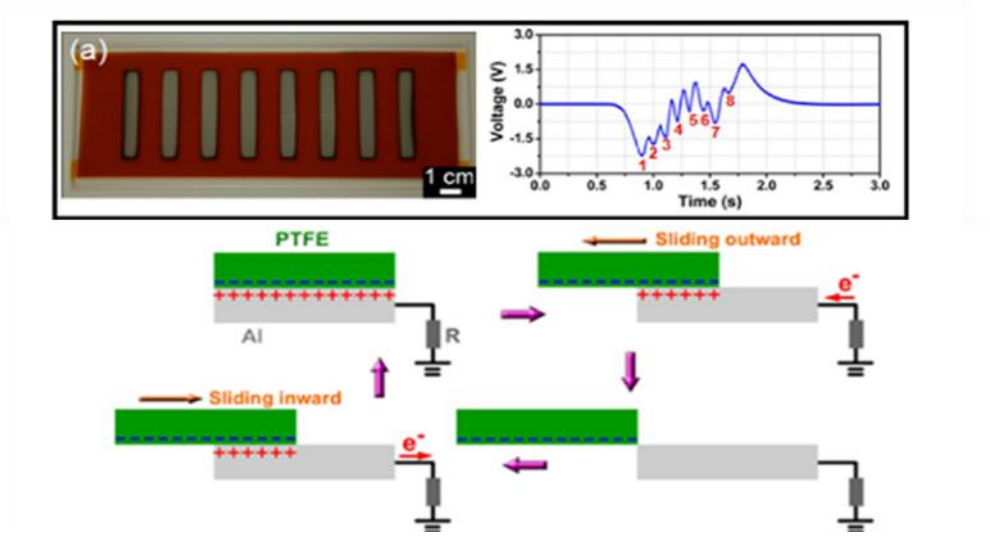

Figure 5. Sliding method [7]

With the same purpose and using the same principle of implementation a device that allows to monitor the position of a steel ball along a tube was built by Yu Su et al. (Figure 6) [8].

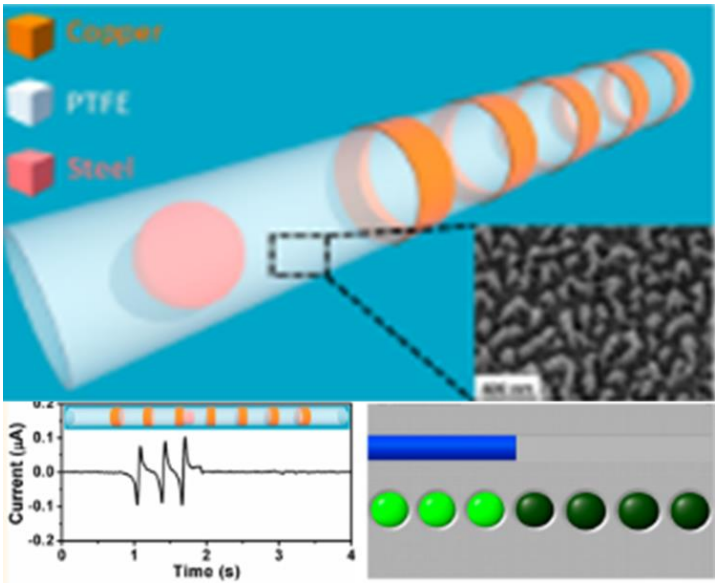

Figure 6. Tracking object inside tubing [8]

The methods of operation of triboelectric can be used for the storage of electrical charges (harvesting energy), allowing feeding small circuits, matching a given electrical potential generated to a given phenomenon or can be used as a sensor, monitoring the position of electrodes

place in a location for monitoring the angular position, angular velocity among other aspects (Figure 7)[9].

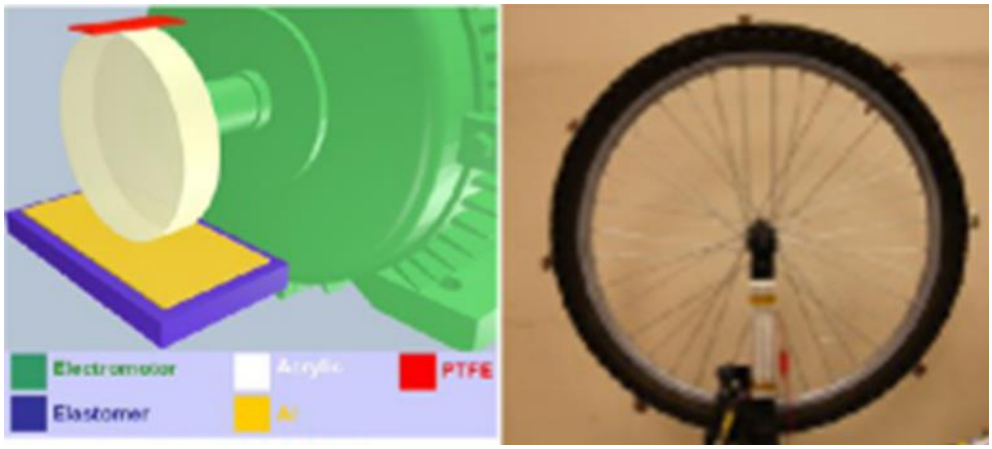

Figure 7. Harvesting energy from a single electrode method [9]

3. Triboelectric materials on electronic skin

As mentioned previously, the different units that allow the monitoring of variables are called sensors allowing their quantification. The analysis of the displacement of leg and arm structures in the analysis of gait and upper limbs. Xuexian Cheng et al. developed an extensible device, in PDMS and PU fiber coated with CNT & AgNWs. This flexible structure allows monitoring the angular position and pressure, as analyzed in Figure 8. This triboelectric device, through PDMS surface in pyramidal form, allows an increase of the relative area, increasing the signal effect along the displacement [10].

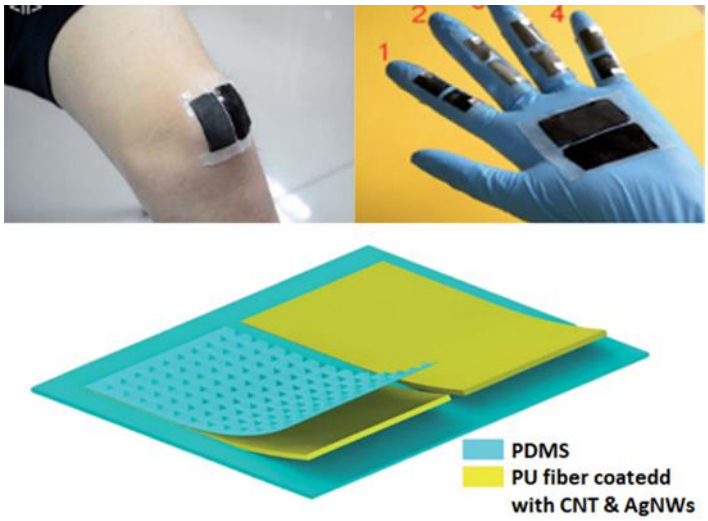

Figure 8. Stretchable e-skin [10]

Other electronic-skins that allow the monitoring of human patterns were reported by Shienho Harada et al [11]. They developed a deformation sensor with the pair of Au NS film embedded in

PDMS and PDMS (Figure 9), with a pyramidal surface with the aim of increasing the contact area between the two electrodes along the deformation [12].

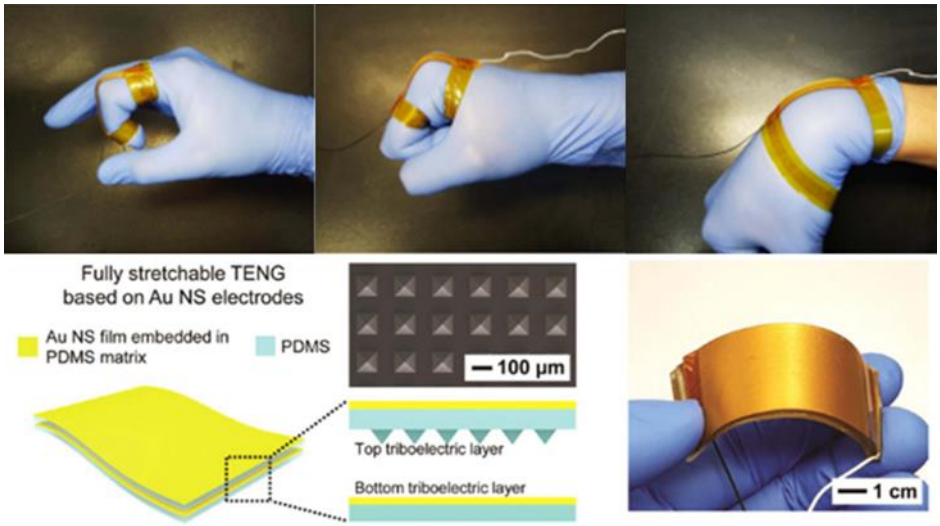

Figure 9. Stretchable human motion detector [13]

Chen- Min Chiu et al. reports through a harvesting energy technique and also using artificial intelligence the recognition of hand gestures for the interpretation of sign language (Figure 10)[14].

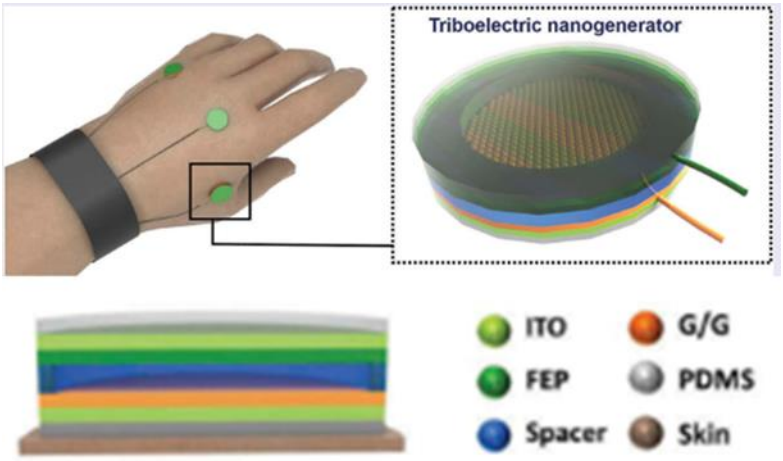

Figure 10. Smart e-skin to gesture recognition and language expression [14]

Also, for incorporation into electronic skins, a system was developed capable of monitoring the contact location and temperature in the contact region (Figure 11). This device was also distributed in a type of two-dimensional array, allowing monitoring the contact site and temperature [11].

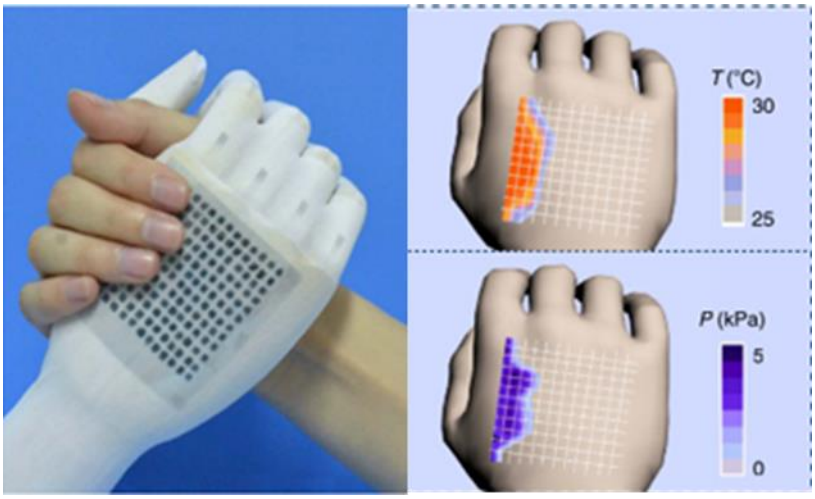

Figure 11. Dual sensor to measure pressure and temperature [15]

An angular analysis of the displacement of the finger around its joint led to the construction of a device that operates with the single electrode method. Thus, Lokesh Dhakar et al., developed an intelligent way to monitor the angular position of the finger joint along the movement (Figure 12). The area between the triboelectric pair depends on the finger position, thus allowing the relationship between the stored energy and the angle between the segments [16].

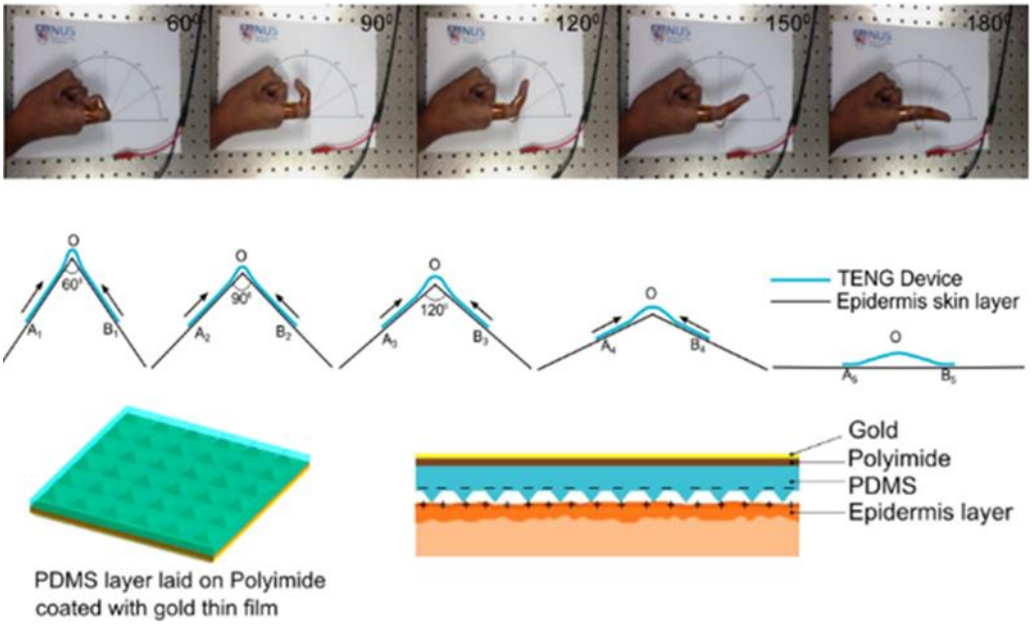

Figure 12. Angle measure by area superposition [17]

4. Traking strategies

The positioning through a device based on a reference position has the counterpart of being necessary an initial calibration and an interpretation of the increment signal that will occur in this monitoring [12], [16]. Take as an example an incremental encoder, where the positioning is given by the number of iterations that is read, added or subtracted from the reference position. So,

Xianjie Pu et al., [18] developed a device that allows monitoring according to a reference position through the sliding method (Figure 13b). Some other strategies were implemented such as increasing the space between the triboelectric strips and read this values alternating with other set of strips as it was shown by Jin Chen et al. [19]. The ease of implementation as well as the simple engineering of this method does not allow the reading of the value corresponding to the angle in real time, requiring processing that can be more complex and time-consuming. The use of an absolute encoder solves some obstacles such as the use of more demanding post-processing and thermite to obtain fastest the angular position (Figure 13a). In contrast, the bit area for production of this strategy will be minimum the larger the total number of bits, establishing an inverse proportionality ratio. Thus, also a resolution will arise that will be smaller the larger the total number of bits.

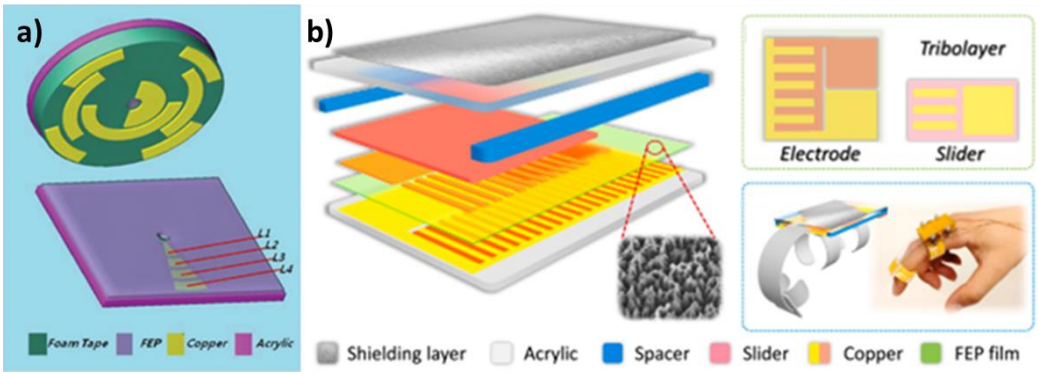

Figure 13. a) encoder to angle measure [20]*; b) Rotation sensing and gesture control* [18]

Independent reading of the different reading bits of the encoder is done using the single electrode mode method (as seen in Figure 4) [19] [21]. The created pattern at the encoder surface will generate a different signal at the reader.

Chapter 3 – Assemble and test of a triboelectric encoder

This chapter will summarize all the activities developed with the purpose of achieving the main objective of this dissertation, from the studies that were carried out to understand the principle of operation of triboelectric to the idealization and elaboration of the sensor.

1. Triboelectric series material position

The triboelectric materials occupy a given position in the triboelectric series. As we saw in chapter 2 this position is imposed according to its relative polarity. As a way of finding that position, it is necessary to have two points of reference in this series, i.e. two materials with already known polarities or a prior record such as that found in Figure 42 in annex. To be introduced to the triboelectric materials different samples were fabricated and testes with a contact separation method.

1.1. Electrical circuits to test triboelectric materials

Two circuits to test triboelectric materials were designed both actuate under the same principles, switching from different components when the triboelectric pair is in contact using one of the principles that was previously seen. The first one allows to calculate the amount of charges that are shared by the triboelectric pair at open circuit conditions by switching from the different capacitors (Figure 14a). The other circuit allowed to obtain the voltage and current provided by the triboelectric pair at a short circuit condition. This provide sufficient data to compute the power which is provided by the tribo-pair depending on the selected load resistance (Figure 14b).

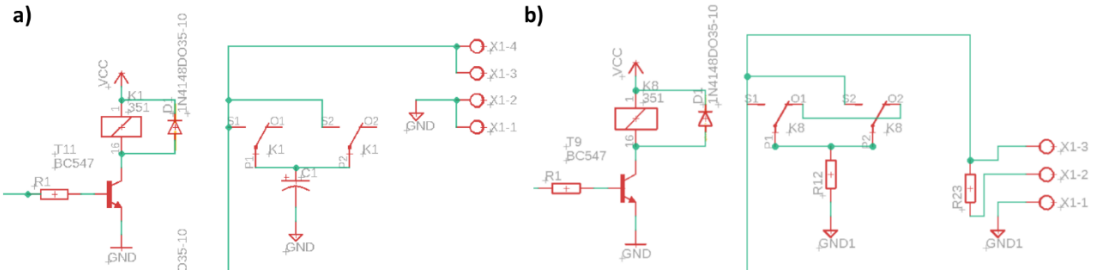

Figure 14. Measurement circuit to test triboelectric materials. a) Charge measurement circuit; b) Voltage, current and power measure circuit

Both circuits were design using EAGLE software that allow to design the circuit as it was showed before and let the user place the electrical components at the board. An automatic algorithm was run to stablish all the connections that latter are printed to a PCB board with dimensions of 161 x 99.55 mm^2, which represent the exact dimensions to be fitted to the isolator box (Figure 15).

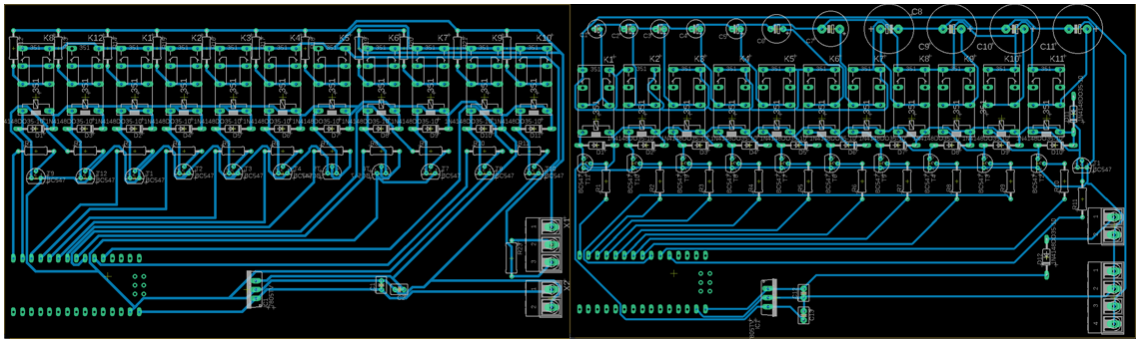

Figure 15. EAGLE software view of the capacitor circuit to the left and the resistance circuit to the right

A mask of the circuits was printed to an acetate and then a PCB and the acetate were expose to a UV light for two minutes. The PCB plate is composed by a photosensitive coat that let the regions without the mask be ionized and then be transferred. After the irradiation time finish the PCB plate was submerged to a caustic soda solution to remove the photosensitive coat that was not protected by the mask. Subsequently it was washed with current water and submerged to a hot solution of iron chlorate and then after all the connection are visible and with a good amount of conductive material it was washed again with current water and let dry (Figure 16). After being dry, all components were welded on the PCB plates.

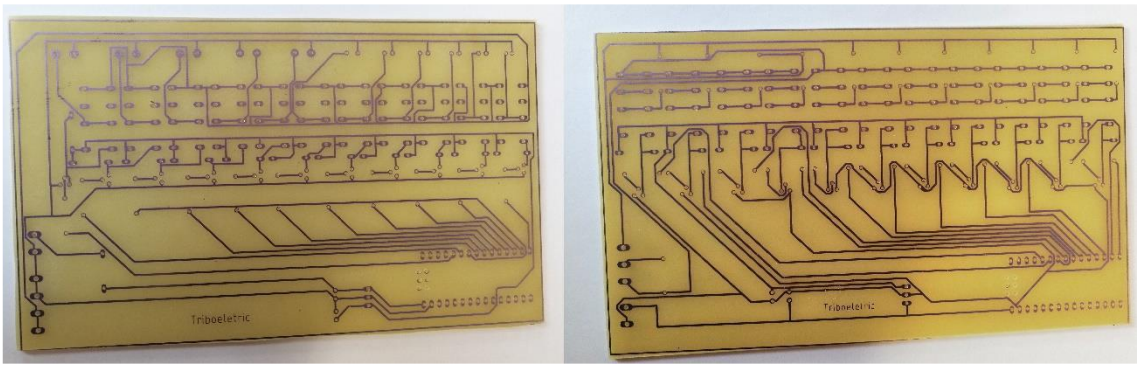

Figure 16. PCB plates, capacitors at left and resistances at right

An antioxidant varnish was them applied for the electrical connections not to be damage by erosion of the environment and oxidation.

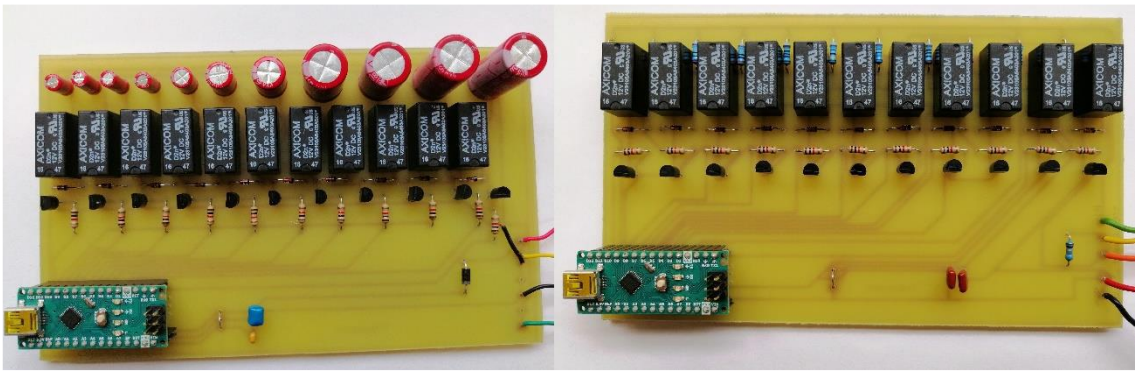

Figure 17. PCB with welded components. at left the capacitors, at right the resistance

During the test of the device previously created, the results were not the ones that were expected. This situation was due to the low value resistance (3 Ω, 12 Ω, 20 Ω, 30 Ω, 100 Ω, 140 Ω, 160 Ω, 200 Ω, 300 Ω, 1 kΩ, 1.6 kΩ;) that was implemented at that circuits. A high value resistance (100 Ω, 1 kΩ, 10 kΩ, 100 kΩ, 470 kΩ, 1 MΩ, 4,7 MΩ, 10 MΩ, 68 MΩ, 100 MΩ, 470 MΩ)for a similar device was then used to collect the data needed.

1.2. Triboelectric materials testing

This first test was carried out to show the influence of annealing temperature and time on the generated electrical power of PTFE films fabrication in a solution of 60wt % dispersion in water. Those samples were cured at different temperatures (200 C, 250 C, 300 C, 320 C, 400 C, 430 ^{o}C) and wires were welded to take measurements (Figure 18).

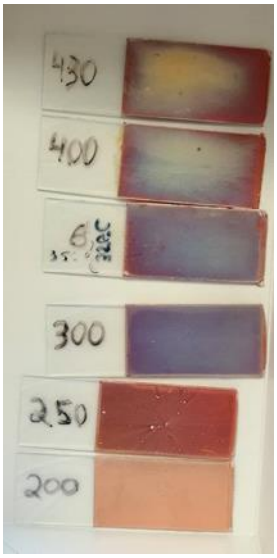

Figure 18. PTFE sample with different annealing temperature

The values to the different temperatures, rotation speed of the spin coating technique, time intervals of the rotation, annealing period and hot plate temperature used to performed these samples are displayed in the Table 1.

Table 1. PTFE spin coating rotation, plate temperature, thermometer temperature and healing period

Test	RPM	T (s)	TempP (°C)	TempT (°C)	Annealing P.
1	1500	30'	200	187	4''11'
2			250	228	3''30'
3			300	274	2''40'
4			350	323	1''15'
5			400	361	45'
6			430	377	38'

Several tests were performed by the contact separation method using a pneumatic system to obtain difference of potential, current and then calculate the power as a function of load resistance. All these samples were tested with a PTFE coated sheet as the second tribo-pair. The results of the different variables in study are showed in Figure 19. Analysing the results, it is visible that the voltage increases and current decrease with the load resistance as well as the annealing temperature, On the other hand, the power of this triboelectric pair reaches a maximum value at 10^7 Ω. These tests were performed twice but several samples were damage by the contact separation-method as it could be seen at the Figure 43 at the attachments of this report.

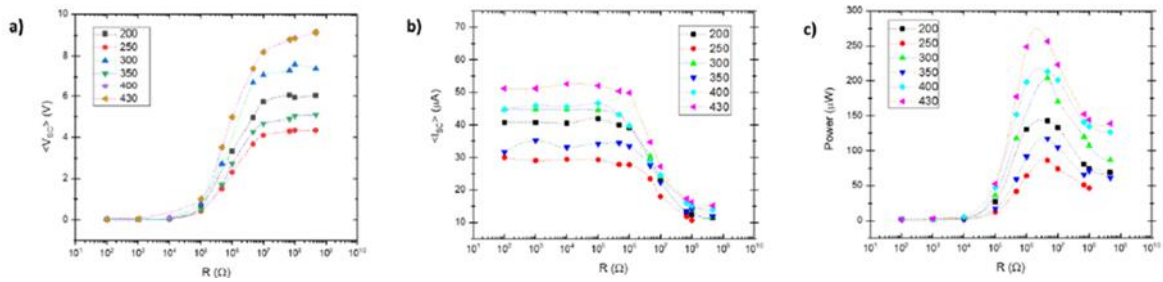

Figure 19. Influence of annealing temperature on voltage (a)), current (b)) and power (c))

The study of the positioning of PLA (material used in 3D printing) in the triboelectric series, we carried out a studies on the reproducibility and validation of the sensor that will be developed. Thus, four rectangular structures (2.5 x 5 cm^2) were printed to begin the intended study. To analyze the influence of the relative area, two different extruder tips different from (0.4 and 0.6 mm) and thicknesses (2 mm and 4 mm) were used. The area of these samples remained constant so that it was possible to compare with the results obtained in the previous study.

Analyzing the results obtained after contact-separation tests it is possible to verify that the thickness of the PLA layer will be inversely proportional to the charges that flow between the pair, that is, the greater the thickness the smaller the charge, so the extruder tip will influence the contact area between the triboelectric pair. However, the data proved to be somewhat inconclusive. For the PTFE-PLA pair, the 0.6 mm extruder tip showed the best results than the 0.4 mm but with the polyamide polymer pair the results were reversed (Figure 20).

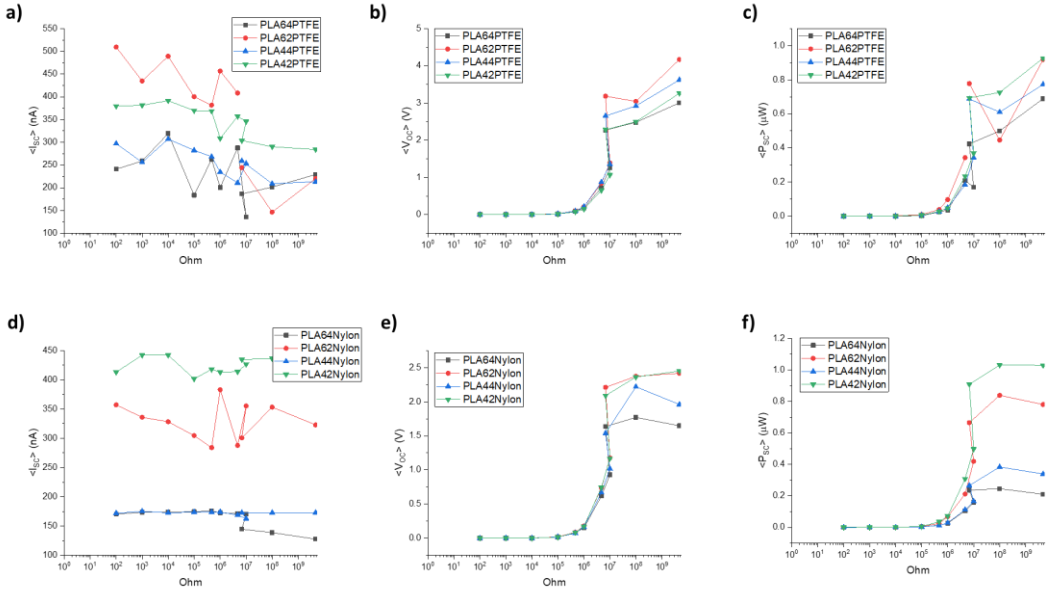

Figure 20. a), b), c)- PLA and PTFE TENG pair; d), e), f)- PLA and Polyamide polymer TENG pair

It was possible to compare with the results obtained previously (Figure 43 attached), where the same tests were performed with polyamide polymer sheet and a solution of 60wt % dispersion in PTFE water, concluding that the PLA is closer to polyamide polymer than PTFE in the

triboelectric series (Figure 21), because it shares less loads with polyamide polymer. These results were confirmed by Shirui Liu et al. report [22].

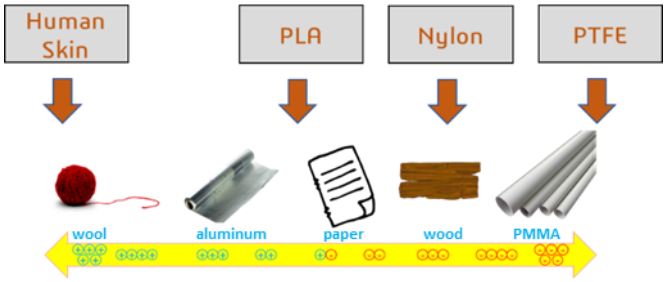

Figure 21. Sorted triboelectric series

2. Encoder

To be able to know the exact position of a given object it is necessary to be aware of the reference positions and obtain an incremental system that indicates the increment each time this increment is captured by the reader [23]. However, this system gives positioning relative to a reference and not the exact position of the structure. Thus, the assignment of an encoding to a given position came to give space to what is known as an absolute encoder, allowing the monitoring of positioning along the movement in real time.

The position is given by a binary word. The number of bits, constituent of this word, is directly related to the resolution of this sensor along the surface. Two encoders were developed, one linear and one rotating using a 7-bit word in Gray code.

2.1. Decimal to Gray conversion

The 7 bits of the binary word give a resolution of 2.81°. Gray code was used that only one bit is changed between two consecutive positions.

To generate the 128 gray words a Python routine was performed that outputs a text file with 3 columns separated by tabs in which the first column contains the decimal number, in the second the code in binary, with the maximum number of bits, and in the third the gray code converted through the second column. This routine was developed in Python and can be found at the annex of this document (page 58). The conversion from binary to gray follows the example of Figure 22

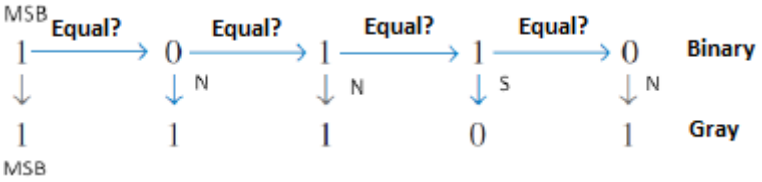

Figure 22. Binary to Gray conversion [24]

2.2.Linear encoder

To start the tests, a linear encoder was created in PLA that will serve as the basis for showing the data that will be collected by the encoder reader through the relief of the surface. SolidWorks was used to create 3D model that gives the ability to be filled in (Figure 23a) and take some measurements with it (Figure 23b)

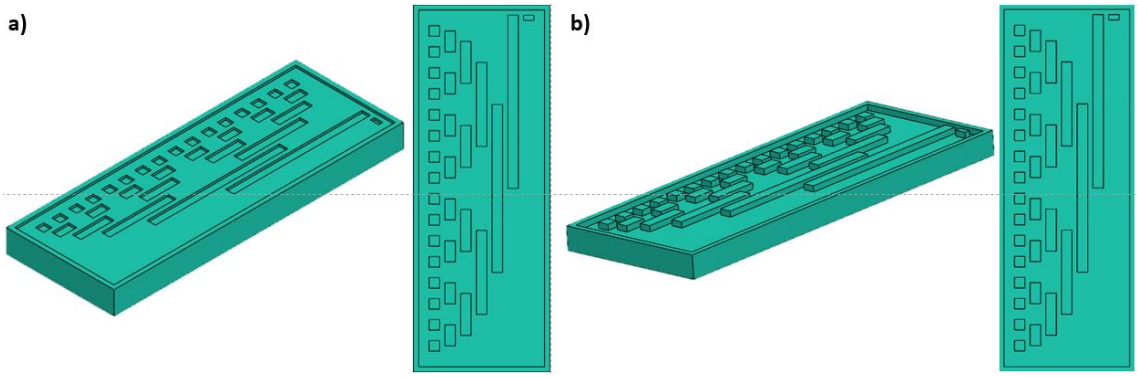

Figure 23. 3D models to the linear encoder- a) PLA mask; b) PLA encoder

To optimize the space, the size of the encoder was reduced, eliminates the existing spaces between each bit. A 3D model was carried out too in SolidWorks (Figure 24).

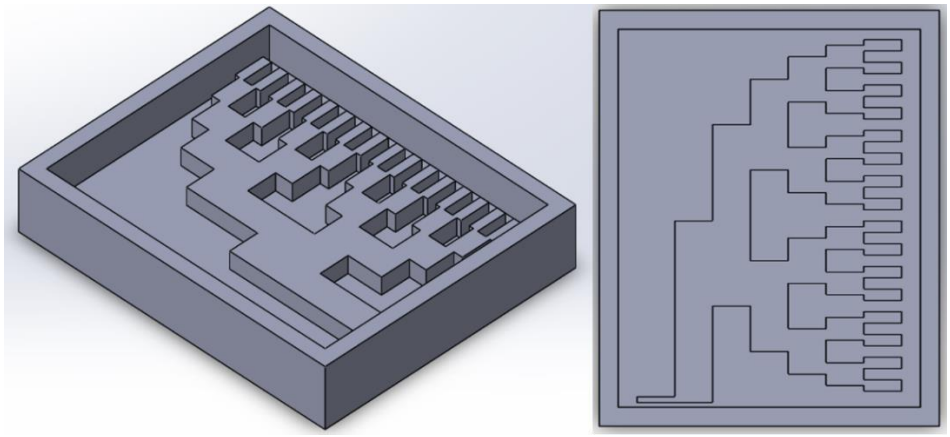

Figure 24. Linear encoder mask to fill with PDMS

2.3.Rotative encoder

Like the encoder developed in the previous two points the rotating component of this same device would be an approach to be studied. Figure 25 shows the rotary encoder drawing with the same number of bits and encoder resolution shown in the preceding points.

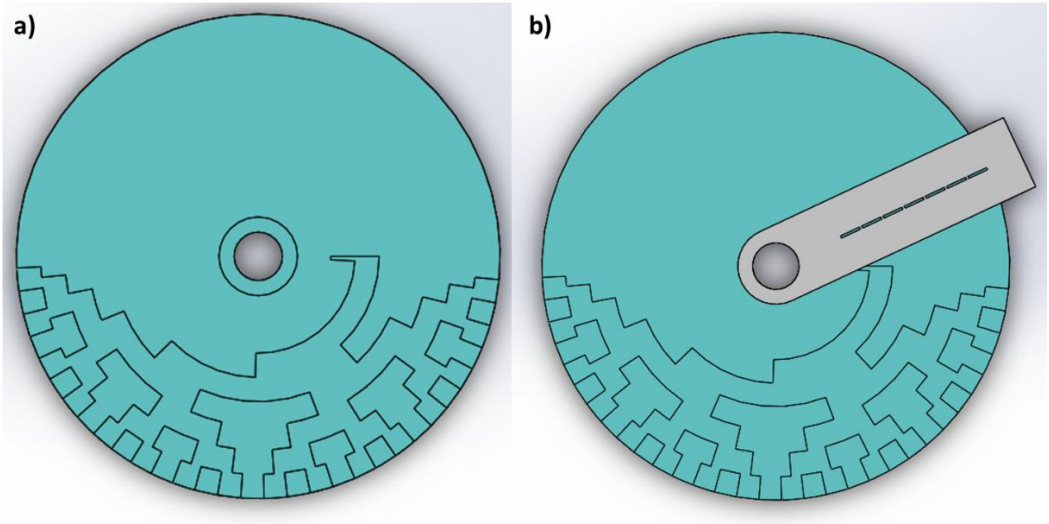

Figure 25. Rotary encoder

The same strategy was implemented in the rotary encoder with the aim of subsequently making an encoder with the same mask (Figure 26).

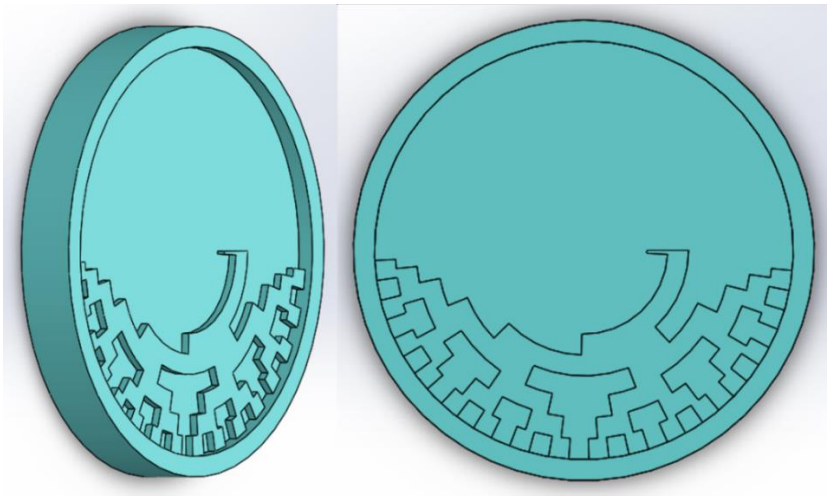

Figure 26. Rotative encoder mask to be filled up

2.4. Flexible encoder

To fabricate a flexible encoder, it is necessary to use a flexibles matrix. PDMS was chosen and to made it, it is necessary to use an elastomer and a curing agent. These two solutions were mixed in the ratio of 10:1, i.e., the curing agent should be 10% of the elastomer. After mixing, the existence of many bubbles in the final product required the use of vacuum to remove them. The mixture was then poured into the mask previously drawn and printed in PLA and then placed in an oven at 85°C for 2 hours. At the end, the PDMS was removed from the mask as can be seen in Figure 27 and it was subject to a plasma using a ETP BD-20V tool to be fixed to a lamella.

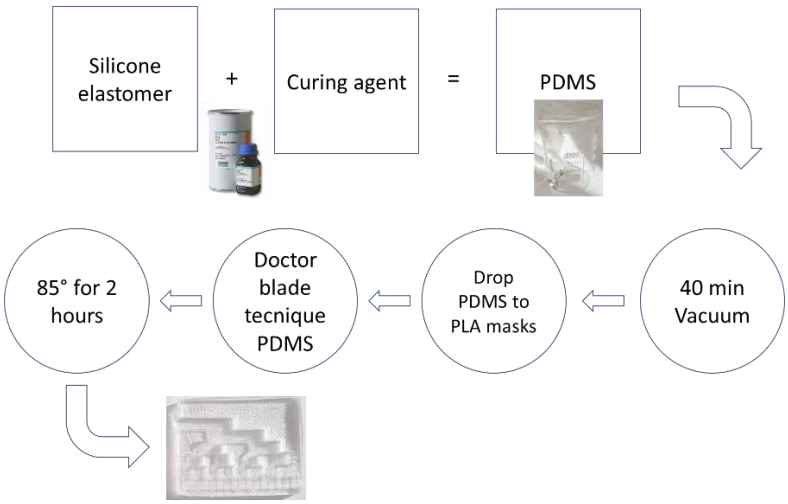

Figure 27. Schematics to obtain a PDMS encoder

3. Encoder reader

To read the data provided by the encoder the surface of the reader needs to be in contact with the encoder surface. Every bit of the encoder should be physically separated from the other ones. SolidWorks was used to design an object that follows all the restrictions (Figure 28)

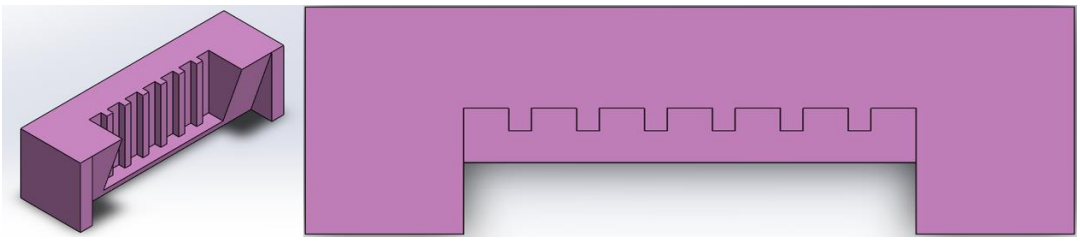

Figure 28. SolidWorks encoder model

The 3D design model was printed, and the bit surfaces was filled with silver paint and a thin wire in order to read the output signal (Figure 29b). Other strategy was applied, and a pattern was design with the exact correspondence of the bits that was created at the previously printed encoder (Figure 29c**Erro! A origem da referência não foi encontrada.**).

Figure 29. Silver electrode implementation. a) PDMS encoder; b) Reader; c) Pattern to be integrated at the encoder

Three materials and implementations were carried out as it could be seen at the Figure 30. These three strategies were used although PE was too thick that was scratched by the encoder.

Polyamide polymer with silver tint, create shortcuts and the signal was not plausible. PTFE shows up the best results keeps its apparency giving a good signal

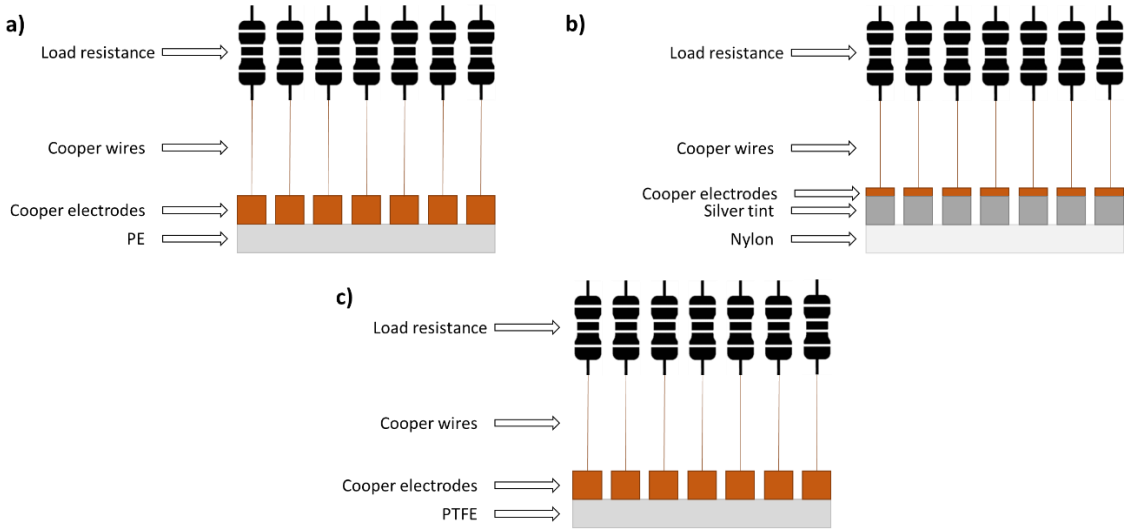

Figure 30. Implementation strategy used to produce signal. a) PE, b) Polyamide polymer with a silver tint coat; c) PTFE

To improve the quality of the signal a coated wire was used to drive the signal to the microcontroller that will collect the data (Figure 31).

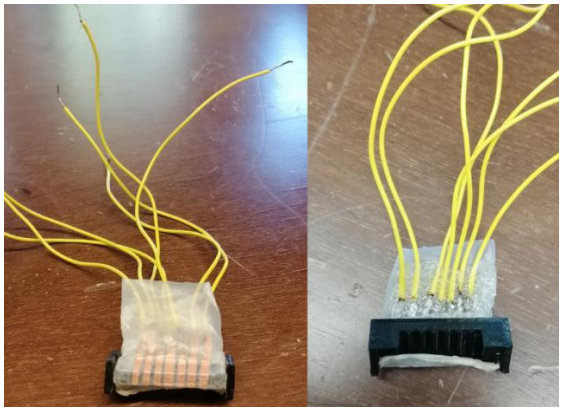

Figure 31. Encoder reader.

4. Signal processing

To obtain data from the reader several aspects have been take in consideration. The triboelectric principle of operation used to collect data from the encoder was the single electrode mode. To use this method the reader the must be kept at the same position and the encoder needs to move at a constant speed. A schematic of this system could be viewed in Figure 32. There is a sliding mechanism which requires a linear motor connected to a *H bridge* and a power supply to move the encoder through the reader. This bridge changes the current orientation that is provided to the engine using four switches. This system allowed to extend and retract the actuator. The data was collected from the Arduino and showed on the computer by serial communication.

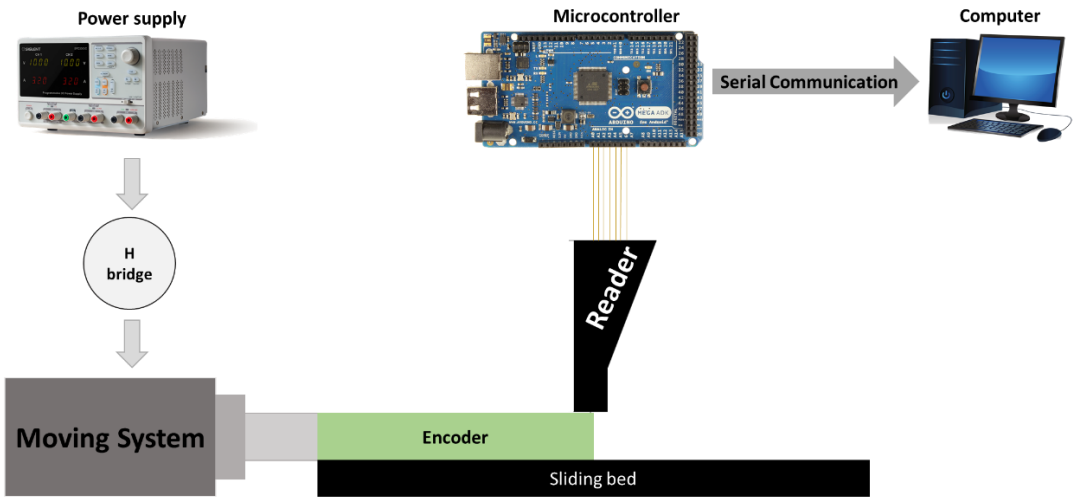

Figure 32. Linear test bench schematics

The implementation of the schematics previously made could be seen at the Figure 33. Increasing the voltage on the power supply one can directly increase the speed of the tool. To calculate the speed of the encoder two yellow strips were positioned at a known distance and every test was filmed. After all tests were performed the speed was calculated in millimetres per second (mms^{-1}).

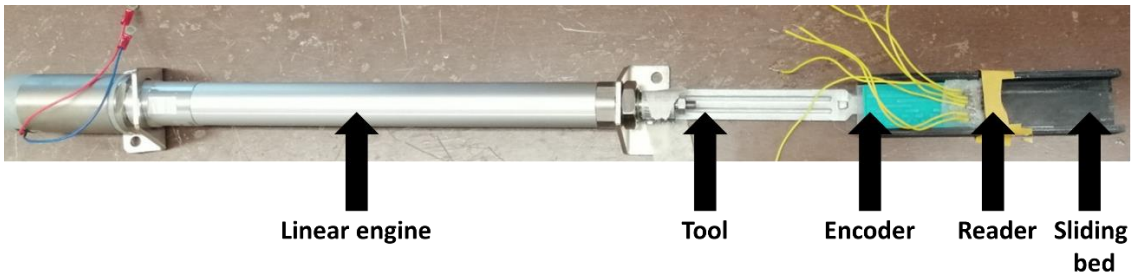

Figure 33. Linear encoder test bench

To read the data from the reader, Arduino was used. Signal wires were connected to the analogical doors of the Arduino, which has an operational amplifier to provide high input impedance, and an ADC, according to the Arduino datasheet [25]. The code that provide the reading of the encoder reader is shown in page 60. No conversation was applied to the incoming data at the code because it would delay the sampling rate of the bits. The incoming data comes at the following format:

<hh:mm:ss:ms> SPACE -> <number of the bit><ADC value>

Data post-processing was performed in Microsoft Excel and exported to Origin. To start data processing the number of samples that every sampling gives to the data collection has to be found. So, the sampling rate of the Arduino was conferred from the datasheet, at this point the number

of samples that must be counted has been reach. This allowed to perform the second task that is to standardize the sample by windowing. This window was calculated by the speed of the encoder and the number of samples as a reason of it. This procedure was made for the three speeds used to keep the integrity of this task and compare graphic behaviours such as monotony.

4.1.Reading only one bit

All the bits were connected at the Arduino's analogic doors although the incoming data was very messy. At this point only one bit was connected to the Arduino and the code was changed to sample one specific bit. This procedure provides a higher sampling rate and a more straightforward result. The selected bit was the fourth most significative bit (Figure 34). One expected a four pike behaviour from the signal because of the four abrupt changes at the encoder pattern.

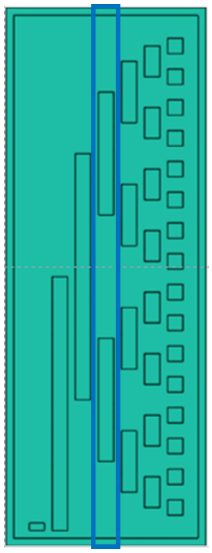

Figure 34. Bit in analyse

As expected for the two different speeds, the pattern that was created to that specific bit has been showed up at the post-processed graph (Figure 35). Here, one shows two different speeds and three different tests. The slowest speed shows a thin spike against the fastest one that shows a more pronounced behaviour.

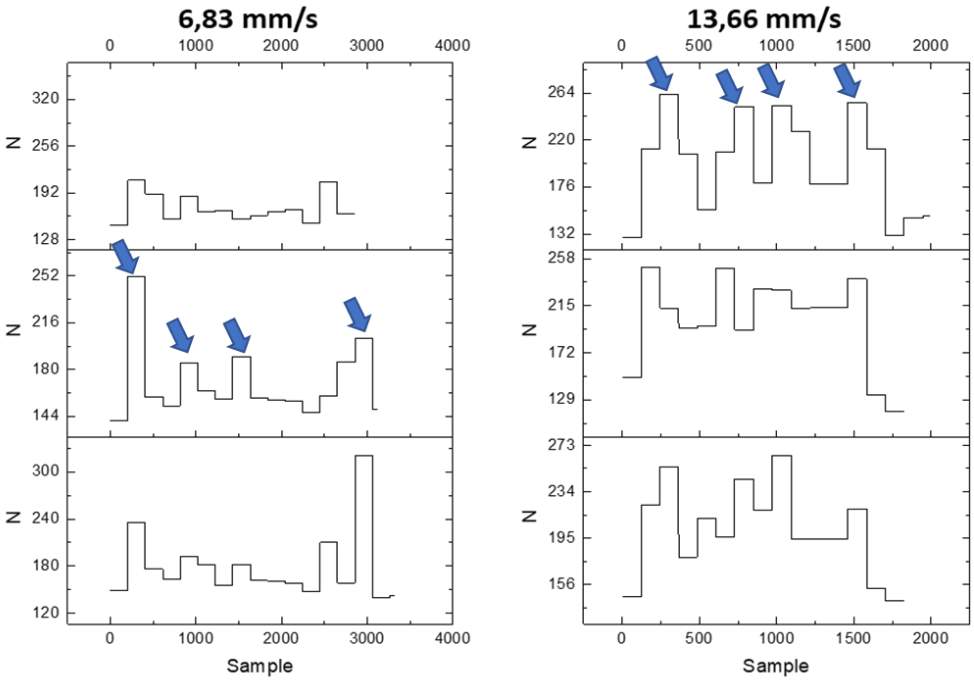

Figure 35. Graphic behaviour of the signal for two speeds

4.2.Reading all bits from the encoder

Instead of the previous procedure, this one requires all the bits to be read at a same time, at a short interval delay. The implemented Arduino code was the most concatenated as possible to reduce the number of iterations between the bit reads. After collecting all data this needs to be split as the time that occurred the reading and the value of that bit. This task was implemented in a C# routine that requires a text file and will create a text file with a 2D matrix with fourteen columns that represents the time and then the ADC value for every bit. The same procedure that was carried before was applied to these 7 bits at the same time. Comparing the results from the previous ones that shows the sampling of only one bit it is possible to understand that the pattern is followed situation. Almost every test performed shows correctly that same pattern, it signifies that same situation could be occurred (Figure 36).

The monotony of the signal remains constant to every of the three-test performed as well as the change of the speed parameter. Some the tests resulted in issues such as the encoder reader lifting when the encoder passes through and does not return to them position. Therefore, more strategies were created to overcome these issues, such as glue the encoder to the support, but they could not slide until the end.

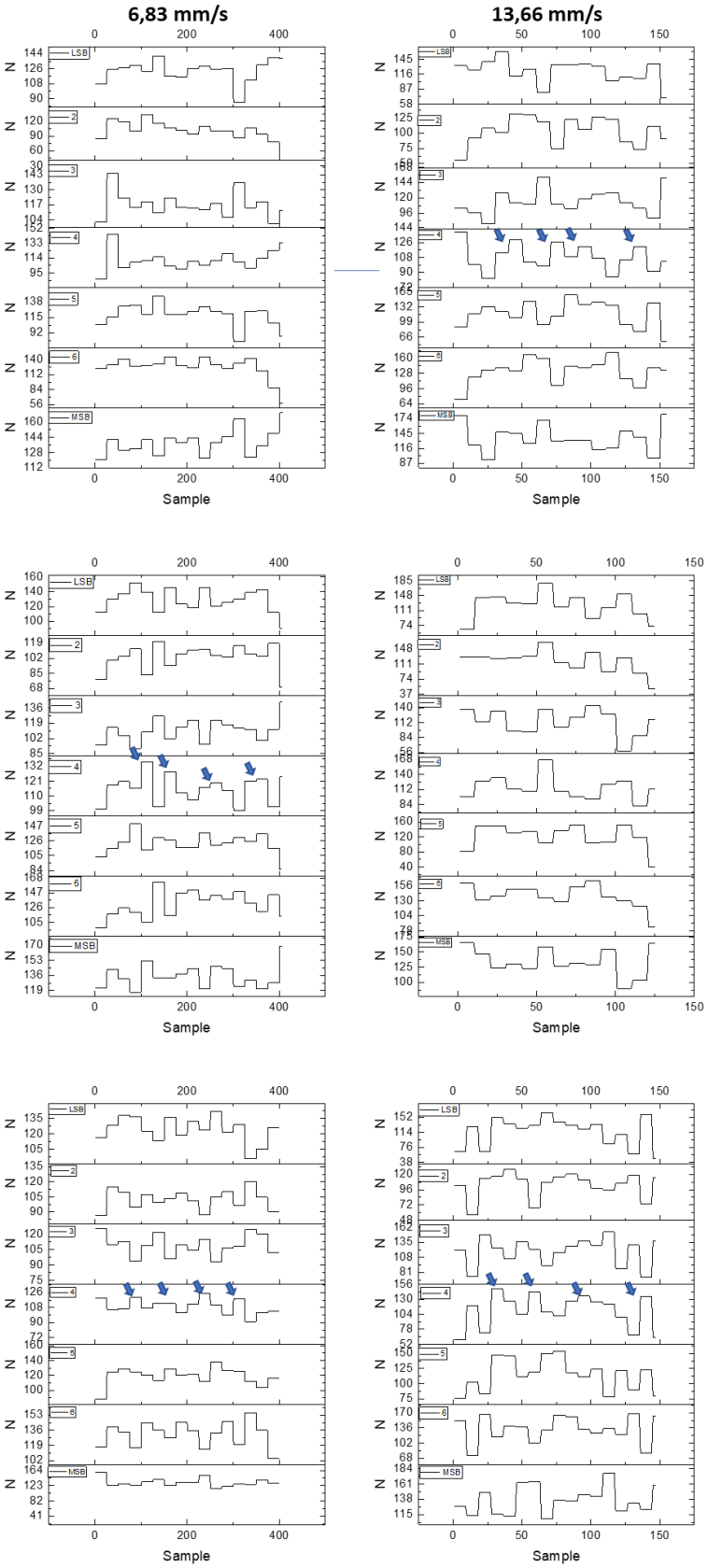

Figure 36.. Graphic behaviour of the 7 bits by two different speeds

5. Angular test bench

To study the triboelectric effect depending on the angle between two structures, the implementation and subsequent validation of the sensor that will be developed, we developed a new test structure. A device consisting of two stepper motors and a controlled Arduino was designed and made through an application created in C#. The schematics represented at Figure 37 show how this system works. This device is designed to move both engines at a given frequency, speed and amplitude according to the user's need (Figure 38a).

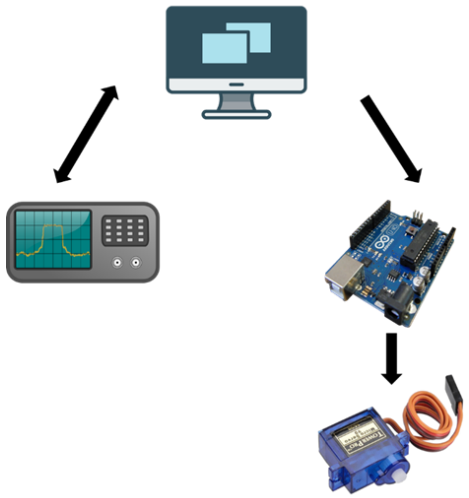

Figure 37. Test bench build schematics

This device was also designed to allow the future incorporation of a human-scale finger prototype (Figure 38b).

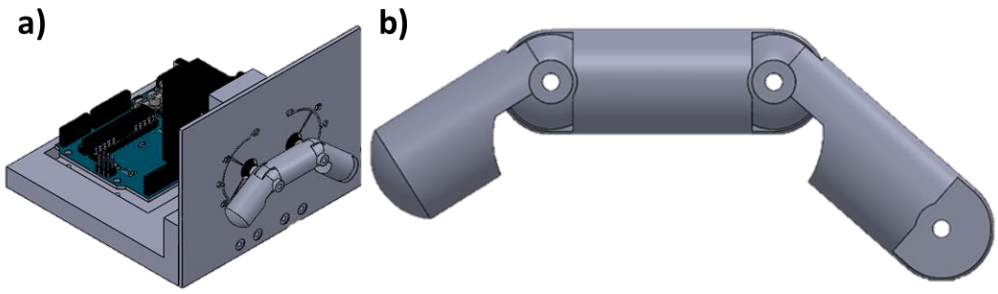

Figure 38. a) Angular test bench; b) Human scale finger prototype

According to some authors, human fingers have dimensions that vary from hand to hand. So, what was possible to accomplish corresponds to the sizing of a middle finger. Based on information from statistical reposts ([26]–[28]) it was possible to sizing a finger that corresponds to the current average dimensions of a human finger. The image in Figure 40 shows the assembled, 3D printed test bench.

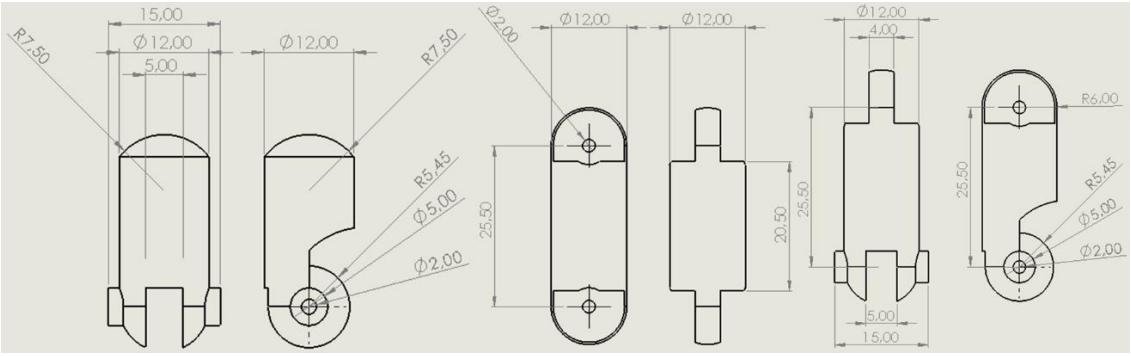

Figure 39. Finger prototype dimension

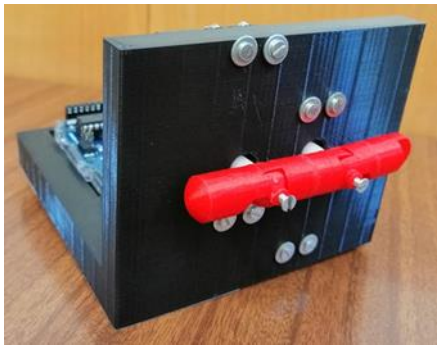

Figure 40. 3D printed test bench

To control this entire system, an application was developed in an object-oriented language, C#. On the left side of the layout (Figure 41) it is possible to control the manipulators by varying the angular displacement interval, oscillation frequency, oscillation joint, and the number of steps of the manipulators. Communication is established between the computer and Arduino to establish parameters through Serial communication, being the microcontroller responsible for decrypting information and maintaining movement.

On the right side of Figure 41 it is possible to obtain the data from the oscilloscope, using a VISA protocol, TekVISANet.dll library [29] provided by equipment manufacturer Tektronix for better communication between the developed software and the device. Among many functions natural of the VISA protocol, it is possible to change the scale of the oscilloscope, calibration and also obtain the values through the command "Curve?" [30]. The graphic values are obtained after the oscilloscope is selected, through the *combobox* that is in the region referring to the control of data acquisition, and then pressed the *Preview Data* button. After being sampled, the values are graphically displayed and the user can save them. If no directory or name is placed and the *Save Data* data store button is pressed, the software will save a .txt file with the values on the desktop with an oscilloscope name followed by the number of identical files that are already in that same directory.

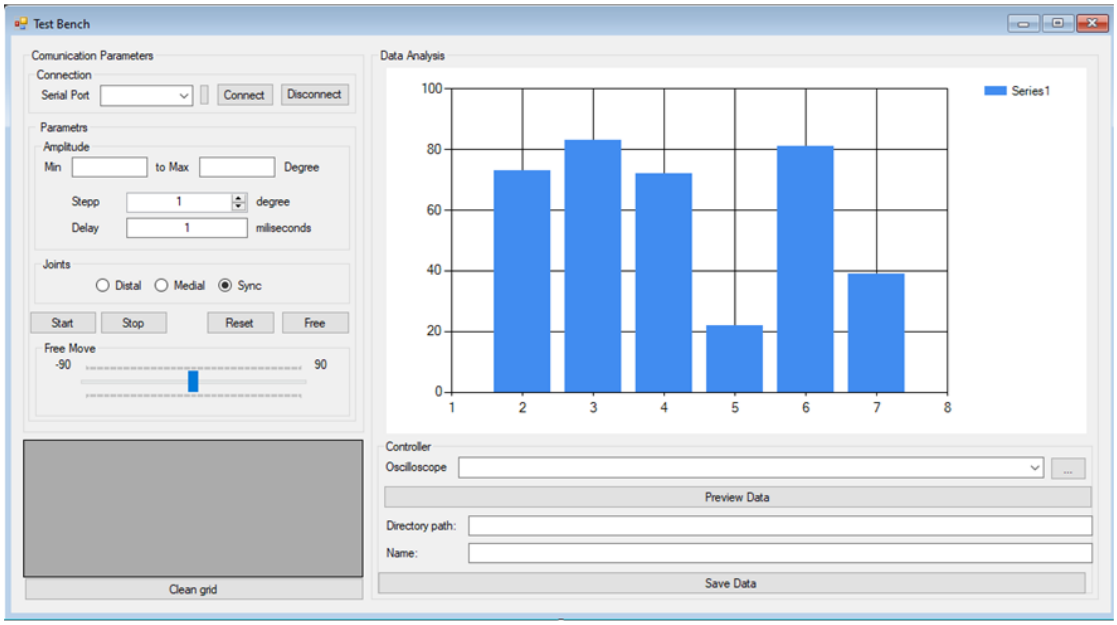

Figure 41. Software Layout

Chapter 4 – Conclusion and future work

This chapter will summarize the work done in this dissertation, regarding the positive as well as the negatives aspects that allowed to build this solution.

1. Summary

The main objective of this dissertation was initially the monitoring the movements of the hand segments, phalanges, monitoring the angle that was between two contiguous segments. This monitoring would be performed using an absolute encoder that would be based on reading the triboelectric effect. The triboelectric pair that was between the reader and the encoder would produce a signal that would be capable, after some processing that could be performed in real time to indicate the absolute position of one segment relative to the other with a resolution of 7 bits or 2.81º. This device would be implemented through a flexible structure that would allow slipping by a reader connected to a microcontroller, or even through a round structure capable of the coupling to the articulation of the segments that would be analyzed.

1.1. Main contributions

The work developed allowed knowledge within the scope of electronic skins, self-power sensors using the triboelectric principle as well as the monitoring systems that were created using this principle. Through the strategies used, the development of a linear encoder that would be read through a surface using triboelectricity was achieved. Thus, signs were obtained that after processing allow the identification of changes in the encoder surface for all bits and it is possible to association a binary word with it.

1.2. Main difficulties

The main difficulties inherent to this project arose in the scarce information that exists about the implementation of specific triboelectric materials in the use of triboelectricity for reading surfaces and how it could be implemented in an encoder. The processing of a signal of such noisy nature often caused the repetition of several tests to which it took time in the development of the sensor. Due to its flexible nature, PDMS was used as a triboelectric pair and due to its viscosity

it was not possible to performed tests with reproducible results because of damaged by the triboelectric pair that was at the other end (PE, Teflon and polyamide polymer).

Also, due to the current circumstances, covid-19 pandemic, the reduction of resources such as access to laboratories, testing, system optimizations and means of machining parts gave way to more improvised solutions such as the test bench for reading the surface of the linear encoder. This linear actuator had an axial clearance that caused the player to be pushed up and not to go back down. It is to be recognized that the positioning of the reader was not the best strategy.

2. Future works

To make all this work feasible, the improvement of some strategies used will be one of the points to be focused. Thus, the design of a new encoder should present a larger spacing to the reading surface, eliminating much of the noise that is applied to the signal. The makeup guides for orientation of the linear actuator movement would cause fewer irregularities in the signal as much as the positioning of the encoder be directed to the slip surface, having the encoder pass over it. A next step would be the implementation of the same principle developed on a rotating surface, as presented. This would require the makeup or printing of the CAD model on a device with higher resolution,

Bibliografia

[1] R. Ribeiro, “Intelligent skin for self-powered hand motion sensing based on triboelectric nanomaterials,” *Wix*, 2020. [Online]. Available: https://up201809054.wixsite.com/website.

[2] X. Wang, L. Dong, H. Zhang, R. Yu, C. Pan, and Z. L. Wang, “Recent Progress in Electronic Skin,” *Adv. Sci.*, vol. 2, no. 10, pp. 1–21, 2015.

[3] K. Xu, Y. Lu, and K. Takei, “Multifunctional Skin-Inspired Flexible Sensor Systems for Wearable Electronics,” *Adv. Mater. Technol.*, vol. 1800628, p. 1800628, 2019.

[4] J. H. Correia and J. P. Carmo, *Introdução à Instrumentação Médica*. 2013.

[5] E. Ramsden, *Hall-effect sensors*, Second Edi. Newnes, 2006.

[6] Dejan, “What is Hall Effect and How Hall Effect Sensors Work,” *How to mechatronics*. [Online]. Available: https://howtomechatronics.com/how-it-works/electrical-engineering/hall-effect-hall-effect-sensors-work/. [Accessed: 26-Nov-2019].

[7] Y. Yang *et al.*, “Single-electrode-based sliding triboelectric nanogenerator for self-powered displacement vector sensor system,” *ACS Nano*, vol. 7, no. 8, pp. 7342–7351, 2013.

[8] Y. Su *et al.*, “Triboelectric sensor for self-powered tracking of object motion inside tubing,” *ACS Nano*, vol. 8, no. 4, pp. 3843–3850, 2014.

[9] H. Zhang *et al.*, “Single-electrode-based rotating triboelectric nanogenerator for harvesting energy from tires,” *ACS Nano*, vol. 8, no. 1, pp. 680–689, 2014.

[10] X. Chen, Y. Song, H. Chen, J. Zhang, and H. Zhang, “An ultrathin stretchable triboelectric nanogenerator with coplanar electrode for energy harvesting and gesture sensing,” *J. Mater. Chem. A*, vol. 5, no. 24, pp. 12361–12368, 2017.

[11] S. Harada, W. Honda, T. Arie, S. Akita, and K. Takei, “Fully printed, highly sensitive

multifunctional artificial electronic whisker arrays integrated with strain and temperature sensors," *ACS Nano*, vol. 8, no. 4, pp. 3921–3927, 2014.

[12] G. H. Lim *et al.*, "Fully strechable and highly durable triboeletric nanogenerator based on gold-nanosheet eletrodes for self powered human-motion detection," 2017.

[13] G. Lim *et al.*, "Nano Energy Fully stretchable and highly durable triboelectric nanogenerators based on gold-nanosheet electrodes for self-powered human-motion detection," *Nano Energy*, vol. 42, no. November, pp. 300–306, 2017.

[14] C. Chiu, S. Chen, Y. Pao, M. Huang, and Z. Lin, "A smart glove with integrated triboelectric nanogenerator for self-powered gesture recognition and language expression," *Sci. Technol. Adv. Mater.*, vol. 20, no. 1, pp. 964–971, 2019.

[15] F. Zhang, Y. Zang, D. Huang, C. A. Di, and D. Zhu, "Flexible and self-powered temperature-pressure dual-parameter sensors using microstructure-frame-supported organic thermoelectric materials," *Nat. Commun.*, vol. 6, no. May, pp. 1–10, 2015.

[16] L. Dhakar, P. Pitchappa, F. E. H. Tay, and C. Lee, "An intelligent skin based self-powered finger motion sensor integrated with triboelectric nanogenerator," *Nano Energy*, vol. 19, pp. 532–540, 2016.

[17] L. Dhakar, P. Pitchappa, F. Eng, H. Tay, and C. Lee, "An intelligent skin based self-powered fi nger motion sensor integrated with triboelectric nanogenerator," *Nano Energy*, vol. 19, pp. 532–540, 2016.

[18] X. Pu *et al.*, "Nano Energy Rotation sensing and gesture control of a robot joint via triboelectric quantization sensor," vol. 54, no. September, pp. 453–460, 2018.

[19] J. Chen *et al.*, "A self-powered 2D barcode recognition system based on sliding mode triboelectric nanogenerator for personal identification," *Nano Energy*, vol. 43, no. November 2017, pp. 253–258, 2018.

[20] Y. Wu *et al.*, "A self powered angle measurement sensor based on triboelectric nanogenerator," *Adv. Funct. Mater.*, vol. 25, no. 14, pp. 2166–2174, 2015.

[21] P. Bai *et al.*, "Transparent and flexible barcode based on sliding electrification for self-powered identification systems," *Nano Energy*, vol. 12, pp. 278–286, 2015.

[22] S. Liu, W. Zheng, B. Yang, and X. Tao, "Triboelectric charge density of porous and deformable fabrics made from polymer fibers," *Nano Energy*, vol. 53, no. July, pp. 383–390, 2018.

[23] Y. Wu *et al.*, “FULL PAPER A Self-Powered Angle Measurement Sensor Based on Triboelectric Nanogenerator,” pp. 2166–2174, 2015.

[24] P. Guimarães, “Eletrónica Digital Capítulo 2 – Sistemas Numéricos e,” pp. 1–68, 2016.

[25] Arduino, “Arduino mega 2560 REV3.” [Online]. Available: https://store.arduino.cc/arduino-mega-2560-rev3.

[26] M. E. R. Nicholls *et al.*, “A new means of measuring index / ring finger (2D : 4D) ratio and its association with gender and hand preference preference,” vol. 0678, 2008.

[27] L. Gillam, R. Mcdonald, F. J. P. Ebling, and T. M. Mayhew, “Human 2D (index) and 4D (ring) finger lengths and ratios : cross-sectional data on linear growth patterns , sexual dimorphism and lateral asymmetry from 4 to 60 years of age,” pp. 325–335, 2008.

[28] H. Mnyusiwalla, P. Vulliez, J. P. Gazeau, and S. Zeghloul, “A New Dexterous Hand based on Bio - Inspired Finger Design For Inside - Hand Manipulation,” no. January, 2015.

[29] Tektronix, “CSharp_Using_TekVISANet_dll.” [Online]. Available: https://www.tek.com/csharp_using_tekvisanet_dll.

[30] “TDS2000 Series Digital Oscilloscopes: Programmer Manual,” *Tektronix*.

Attachment

Extended triboelectric series

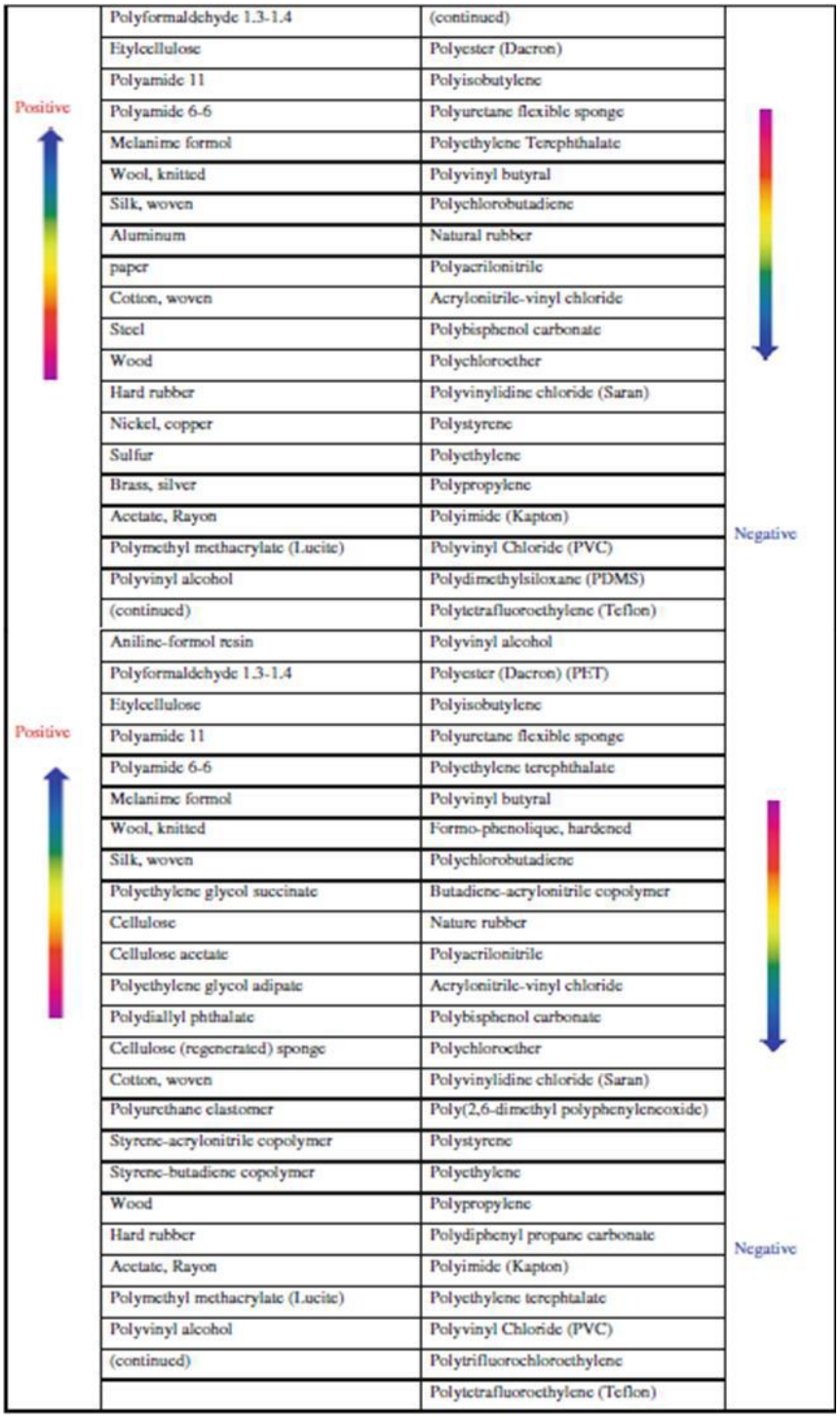

Polyformaldehyde 1.3-1.4	(continued)
Etylcellulose	Polyester (Dacron)
Polyamide 11	Polyisobutylene
Polyamide 6-6	Polyuretane flexible sponge
Melanime formol	Polyethylene Terephthalate
Wool, knitted	Polyvinyl butyral
Silk, woven	Polychlorobutadiene
Aluminum	Natural rubber
paper	Polyacrilonitrile
Cotton, woven	Acrylonitrile-vinyl chloride
Steel	Polybisphenol carbonate
Wood	Polychloroether
Hard rubber	Polyvinylidine chloride (Saran)
Nickel, copper	Polystyrene
Sulfur	Polyethylene
Brass, silver	Polypropylene
Acetate, Rayon	Polyimide (Kapton)
Polymethyl methacrylate (Lucite)	Polyvinyl Chloride (PVC)
Polyvinyl alcohol	Polydimethylsiloxane (PDMS)
(continued)	Polytetrafluoroethylene (Teflon)
Aniline-formol resin	Polyvinyl alcohol
Polyformaldehyde 1.3-1.4	Polyester (Dacron) (PET)
Etylcellulose	Polyisobutylene
Polyamide 11	Polyuretane flexible sponge
Polyamide 6-6	Polyethylene terephthalate
Melanime formol	Polyvinyl butyral
Wool, knitted	Formo-phenolique, hardened
Silk, woven	Polychlorobutadiene
Polyethylene glycol succinate	Butadiene-acrylonitrile copolymer
Cellulose	Nature rubber
Cellulose acetate	Polyacrilonitrile
Polyethylene glycol adipate	Acrylonitrile-vinyl chloride
Polydiallyl phthalate	Polybisphenol carbonate
Cellulose (regenerated) sponge	Polychloroether
Cotton, woven	Polyvinylidine chloride (Saran)
Polyurethane elastomer	Poly(2,6-dimethyl polyphenyleneoxide)
Styrene-acrylonitrile copolymer	Polystyrene
Styrene-butadiene copolymer	Polyethylene
Wood	Polypropylene
Hard rubber	Polydiphenyl propane carbonate
Acetate, Rayon	Polyimide (Kapton)
Polymethyl methacrylate (Lucite)	Polyethylene terephtalate
Polyvinyl alcohol	Polyvinyl Chloride (PVC)
(continued)	Polytrifluorochloroethylene
	Polytetrafluoroethylene (Teflon)

Figure 42. Extended triboelectric series

Python code to Binary to Gray convertion

```
nOfBits=7

minValue=0

maxValue=64

def str_append(s,n):

    output=''

    i=0

    while i<n:

        output+=s

        i=i+1

    return output

f=open("convertion.txt","w+")

f.write("Decimal\tBinary\tGray\n)

for I in range (min Value, max Value+1):

    frontHandZeros=str_append("0", nOfBits-len(bin(i)[2:]))

    binaryWord=frontHandZeros+bin(i)[2:]

    grayWord=binaryWord[0]

    for j in range (1, len(binaryWord)):

        if binaryWord[j-1] == binaryWord[j]:

            grayWord+="0"

        else:

            grayWord+="1"

    print(str(i)+"\t"+binaryWord+"\t"+grayWord)

    f.write(str(i)+"\t"+binaryWord+"\t"+grayWord+"\n")

f.close()
```

PTFE and Polyamide polymer tests

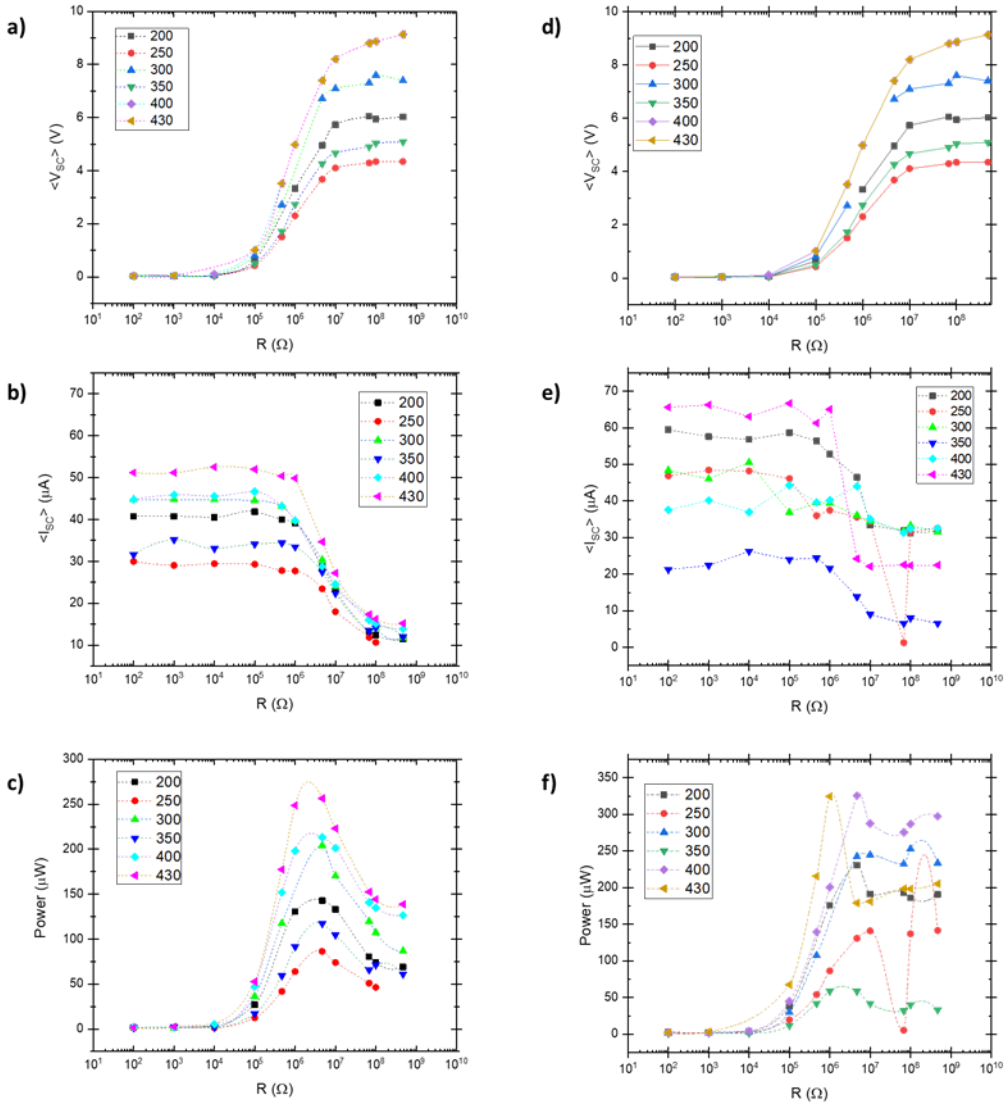

Figure 43. Influence of annealing temperature on voltage, current and power. a), b) and c) represents the first test and d), e) and f) represent the second test.

Arduino data collected code from the encoder reader

```
void setup() {
  Serial.begin(9600);
}
void loop() {
  Serial.print("1 "); //MSB
  Serial.println(analogRead(A0));
  Serial.print("2 ");
  Serial.println(analogRead(A1));
  Serial.print("3 ");
  Serial.println(analogRead(A2));
  Serial.print("4 ");
  Serial.println(analogRead(A3));
  Serial.print("5 ");
  Serial.println(analogRead(A4));
  Serial.print("6 ");
  Serial.println(analogRead(A5));
  Serial.print("7 "); //lsb
  Serial.println(analogRead(A6));
}
```